

LETTERS

Single-cell NF- κ B dynamics reveal digital activation and analogue information processing

Savaş Tay^{1,2*}, Jacob J. Hughey^{1*}, Timothy K. Lee¹, Tomasz Lipniacki³, Stephen R. Quake^{1,2} & Markus W. Covert¹

Cells operate in dynamic environments using extraordinary communication capabilities that emerge from the interactions of genetic circuitry. The mammalian immune response is a striking example of the coordination of different cell types¹. Cell-to-cell communication is primarily mediated by signalling molecules that form spatiotemporal concentration gradients, requiring cells to respond to a wide range of signal intensities². Here we use high-throughput microfluidic cell culture³ and fluorescence microscopy, quantitative gene expression analysis and mathematical modelling to investigate how single mammalian cells respond to different concentrations of the signalling molecule tumour-necrosis factor (TNF)- α , and relay information to the gene expression programs by means of the transcription factor nuclear factor (NF)- κ B. We measured NF- κ B activity in thousands of live cells under TNF- α doses covering four orders of magnitude. We find, in contrast to population-level studies with bulk assays², that the activation is heterogeneous and is a digital process at the single-cell level with fewer cells responding at lower doses. Cells also encode a subtle set of analogue parameters to modulate the outcome; these parameters include NF- κ B peak intensity, response time and number of oscillations. We developed a stochastic mathematical model that reproduces both the digital and analogue dynamics as well as most gene expression profiles at all measured conditions, constituting a broadly applicable model for TNF- α -induced NF- κ B signalling in various types of cells. These results highlight the value of high-throughput quantitative measurements with single-cell resolution in understanding how biological systems operate.

Most of the information on cell signalling has been obtained from population-level studies using bulk assays, yet it is not clear if population data faithfully reflect how individual cells respond^{4,5}. For example, pulsed responses of p53 to radiation damage are evident only at the single-cell level⁶, and are blurred out in population measurements. Similarly, recent studies of lipopolysaccharide-induced NF- κ B activity showed that only half of cells responded to the secondary TNF- α autocrine signal, creating distinct subpopulations^{7,8}. Determining variation at the single-cell level is a powerful tool both for understanding drug response⁹ and for general understanding of how biological systems work, and single-cell culture measurements often complement *in vivo* studies where cells reside in more complex contexts.

To investigate how individual cells respond to variation in input signal level, we studied nuclear localization dynamics of the transcription factor NF- κ B under stimulation with the inflammatory signalling molecule TNF- α . NF- κ B controls the expression of hundreds of genes in response to a wide range of stimuli including signalling molecules, and pathogens such as bacteria and virus¹⁰. The dysregulation of NF- κ B is involved in chronic infection, cancer, inflammatory disease, autoimmune disease and improper immune system development¹¹. Population studies² have not revealed the intricate network of

information one observes at the single cell level^{8,12,13}. Previous time-dependent single-cell experiments were limited to high TNF- α concentrations (10 ng ml^{-1}) and relatively small numbers of cells. Single-cell NF- κ B pathway activation and dynamic properties at lower doses have therefore remained an open question.

We cultured 3T3 mouse fibroblast cells⁸ in a microfluidic cell culture platform³ to measure NF- κ B activity under ten different TNF- α concentrations (100 ng ml^{-1} to 0.005 ng ml^{-1}) with single-cell resolution (Supplementary Fig. 1). Upon stimulation, NF- κ B was transported from the cytoplasm to the nucleus and back out again in characteristic oscillations which we observed with a fluorescent fusion protein (Supplementary Movies 1 and 2). The microfluidic system mimics physiological conditions in terms of volume, fluid flow and number of ligands more plausibly than conventional culture environments where secreted signalling molecules are quickly diluted into millilitres of media. More than 400 live cells were quantified at each condition (Fig. 1) and each experiment was repeated four times, extending the throughput of previous such measurements by more than an order of magnitude (Supplementary Table 1). In parallel experiments with conventional (population based) culture, we used real-time quantitative polymerase chain reaction (qPCR) and digital-PCR to quantify time-dependent expression profiles of 23 target genes under the same concentration range to link NF- κ B dynamics to transcriptional activity.

Our measurements reveal the response characteristics of cells at different signal intensities (that is, external TNF- α concentration). One of the most intriguing findings is the discrete nature of single-cell activation: not all cells responded to TNF- α (Fig. 1a, Supplementary Fig. 2 and Supplementary Movies 1 and 2), and the fraction of activated cells decreased with decreasing TNF- α dose (Fig. 1b). Although nearly all of the cells are activated at doses above 0.5 ng ml^{-1} , the percentage of responding cells fell below 50% for 0.1 ng ml^{-1} and fell to 3% at 0.01 ng ml^{-1} . The mean fraction of activated cells of four experiments ($N = \sim 5,000$ single cells) is well described by a Hill function with $n = 1.5$. The activated single-cell traces can be seen in Fig. 1c–f. Notably, the mean area under the first peak for activated cells remained constant over the entire range of concentrations (Fig. 1g), showing that the total NF- κ B nuclear activity was equal during the primary response to the signal, indicating digital activation in response to TNF- α . Similarly, the median peak nuclear intensity changed by only a factor of four in response to a four order of magnitude reduction of the TNF- α concentration (Fig. 1h and Supplementary Fig. 3).

To determine whether the heterogeneous cell activation is entirely based on a pre-existing variation in cell sensitivities^{14,15} (extrinsic noise¹⁶), we stimulated the cells with two 20-min-long pulses of intermediate dose (0.1 ng ml^{-1}) TNF- α , while allowing the cells to reset by giving a 180-min break between pulses¹³. Ten per cent of the cells responded to only the first pulse (Fig. 1j), 9% responded to only

¹Department of Bioengineering, Stanford University, Stanford, California 94305, USA. ²Howard Hughes Medical Institute, Stanford, California 94305, USA. ³Institute of Fundamental Technological Research, Warsaw 02-106, Poland.

*These authors contributed equally to this work.

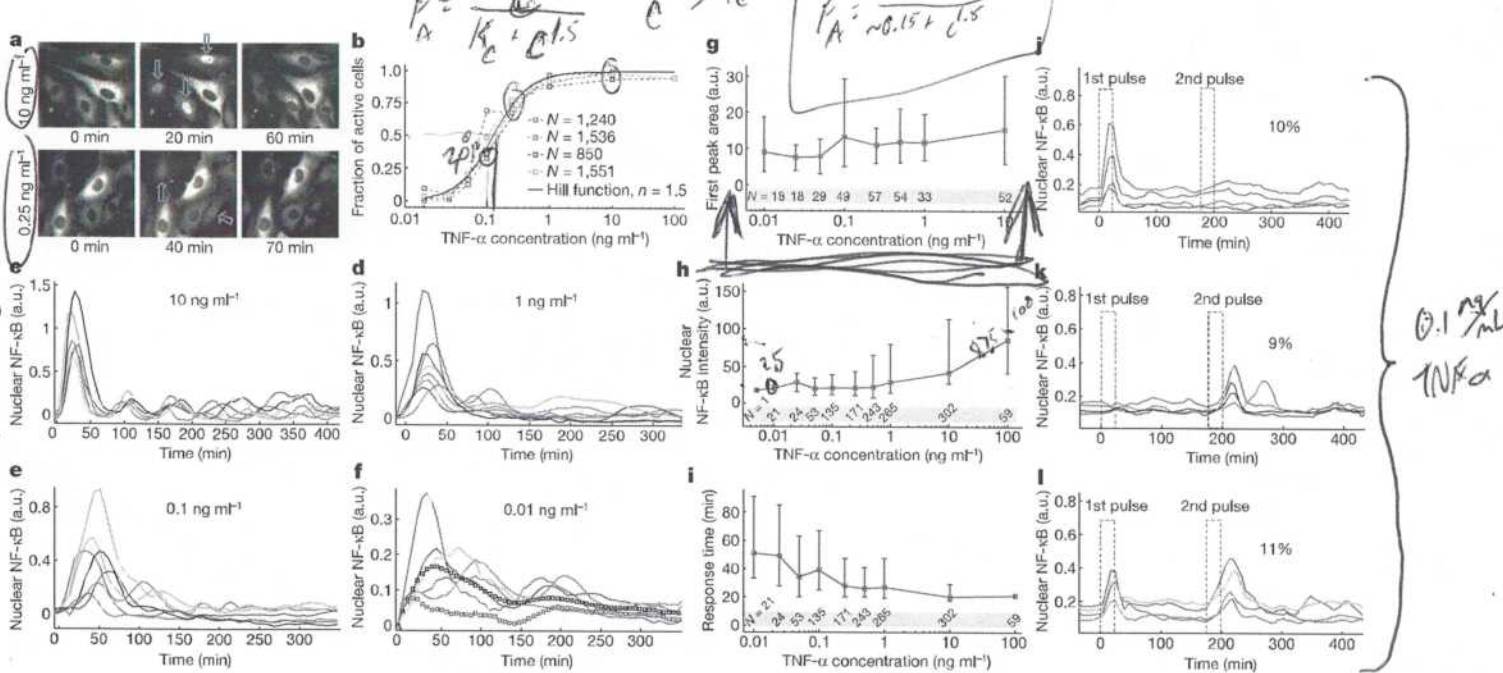


Figure 1 | NF-κB single-cell microscopy measurements. **a**, Representative real-time fluorescent images of cells during stimulation with 10 ng ml^{-1} (top row) and 0.25 ng ml^{-1} (bottom row) TNF- α . Arrows show the activated cell nuclei. At the high dose, all cells except one respond, whereas only two out of five respond at the lower dose. **b**, Fraction of activated cells versus TNF- α concentration for four different experiments (N = number of quantified active cells). The mean of four experiments fit to a Hill function with $n = 1.5$. **c–f**, Representative traces for active single cells. Also shown (f) are population means at 0.01 ng ml^{-1} TNF- α stimulation, when only active cells are included (black squares), and when both active and non-active cells are included (red squares). The population traces averaged over all cells ($N = \sim 80$) misleadingly shows reduced activity. **g**, The integrated area under the first peak versus TNF- α concentration for a single experiment, showing that the total NF-κB nuclear activity in the first peak remains constant across all

the second pulse (Fig. 1k), and 11% responded to both pulses (Fig. 1l). The existence of cells responding to only one of the pulses shows that the activation is governed partly by a stochastic element. However, the probability of responding to both pulses is highly increased (~ 10 fold) compared to a purely stochastic process, which suggests that pre-existing variation in internal variables of the cells (extrinsic noise) also has an important role in the outcome^{14,15}. The heterogeneous activation of single cells requires the re-interpretation of previous population-level studies² and the models derived from them. The population average of only active cells yields an accurate mean nuclear NF-κB intensity (Fig. 1f, black squares). On the other hand, the average over the entire population including active and inactive cells shows significantly reduced mean intensity and completely washed out dynamics (red squares), highlighting the importance of single-cell measurements.

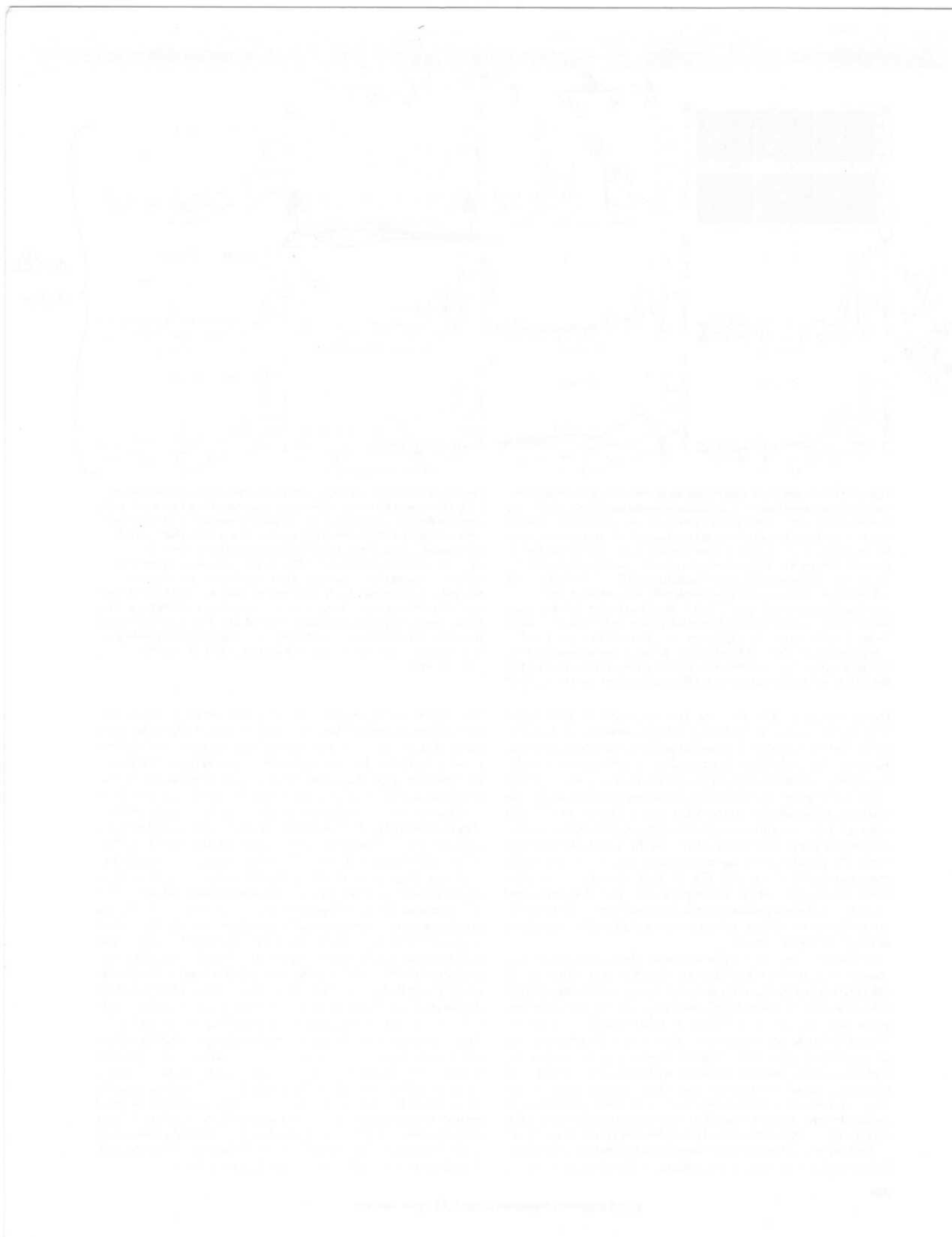
Although the cells show digital activation, there are aspects of their response that are dose-dependent and therefore represent analogue information processing of the stimulus. The cells show significantly delayed activation under lower doses (Fig. 1i). The activation response time (the time from TNF- α stimulation to the first peak) is around 50 min for the lowest doses, whereas the cells activate within 20 min at the highest doses. The variation in response time at the highest doses is close to the experimental resolution of 6 min, and increases to about 60 min at the lower doses. In contrast to the response time, the mean decay time of the first nuclear localization peak (which depends on newly made IκB protein) is around 20 min, and is surprisingly independent of the TNF- α dose (Supplementary Fig. 4).

A related dose-dependent parameter is the number of nuclear oscillations: higher doses yield more oscillations (Supplementary Fig. 5).

concentrations. **h**, NF-κB nuclear intensity versus TNF- α concentration. **i**, NF-κB response time versus TNF- α concentration. Error bars in **g–i** are the standard deviation from the mean, and show the natural variation in single-cell responses. **j–l**, Representative traces for the low-dose, short-pulsed stimulation experiment. Cells were stimulated with two consecutive 20-min-long pulses of 0.1 ng ml^{-1} TNF- α . The pulses were separated by 180 min, allowing the cells to reset. Ten per cent respond to only the 1st pulse (j), 9% respond only to the 2nd pulse (k), and 11% of the cells in the chamber respond to both pulses (l). The existence of cells responding to only one of the pulses indicates that NF-κB activation is partly governed by a stochastic process, whereas the high percentage of cell responding to both pulses indicates pre-existing high sensitivity to TNF- α in this subpopulation.

The intensity of the secondary NF-κB peaks remains relatively constant at high and intermediate doses (Supplementary Fig. 6), but completely disappear in some cells at the lowest doses measured. The time between the first and second peaks remained constant at 80 min over the measured range (Supplementary Fig. 7). Later peaks quickly lose synchrony, and the significant de-phasing after the third peak results in washing-out of the single-cell dynamics at the population level (Supplementary Fig. 3). These subtle variations in the dose-dependent response provide strong constraints on mathematical models of TNF- α -induced NF-κB signalling, which are discussed in more detail below.

At saturating doses of TNF- α , NF-κB nuclear oscillations drive expression of three classes of genes: early, intermediate and late^{12,13,17–19}. We measured the time-dependent expression levels of 23 NF-κB target genes on populations of cells from these classes under a broad range of TNF- α doses using qPCR and digital-PCR²⁰ (Fig. 2 and Supplementary Fig. 8). A series of genes are upregulated at early times, including NF-κB inhibitors *IκBz* (also called *Nfkbia*) and *A20* (also called *Tnfaip3*) (Fig. 2a). Transcripts of early genes often have high degradation rates¹⁸, which resulted in expression profiles that closely follow NF-κB nuclear localization dynamics (Supplementary Fig. 9). An intriguing property of the early-expressed genes is that the expression levels normalized to the fraction of active cells in each population are relatively constant for all doses (Fig. 2b), whereas late genes are only expressed at the highest doses (Fig. 2c). This suggests that the initial NF-κB localization burst is sufficient to express the early genes even at the lowest stimulation doses, linking digital signalling to early gene expression. *IκBz* is one of the digitally expressed genes, which could also explain the dose-independent behaviour of the first peak degradation time we observed in Supplementary Fig. 4.



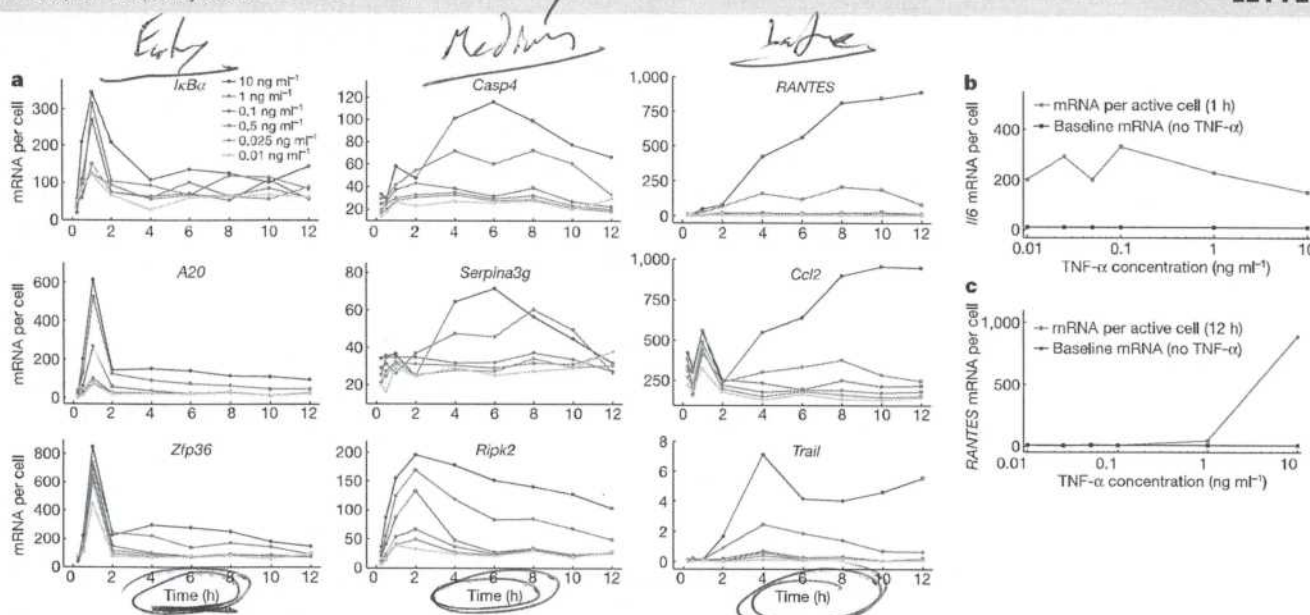


Figure 2 | Time-dependent expression profiles of NF-κB target genes. Cells were stimulated with various doses of TNF- α ranging from 10 ng ml^{-1} to 0.01 ng ml^{-1} . **a**, Relative expression levels of each gene were quantified using approximately 500 cells by qPCR, and digital-PCR was used to calibrate expression levels to the total number of mRNAs per cell. The expression levels shown in **a** are population averages of all cells (active and non-active) in the PCR reaction. Genes cluster in three groups with early (left column), intermediate (middle) and late term (right) activation dynamics.

The expression levels of the intermediate and late genes build up slowly after persistent NF-κB oscillations. Such oscillations require constant TNF- α stimulation and thus are observed only when the initial TNF- α level is highest; at low initial concentrations TNF- α quickly disappears from the media due to natural degradation and receptor internalization (Supplementary Fig. 10). The initial localization peak seen in all active cells is not sufficient to induce the late genes (Fig. 2 and Supplementary Fig. 9). Among the late genes that are highly expressed, *Ccl2*, *Trail* (also called *Tnfsf10*), *Casp4*, *Ripk2* and *RANTES* (also called *Ccl5*) lead to apoptotic signalling and *Serpina3g* acts to prevent apoptosis²¹. This suggests that cells that are continuously exposed to high-dose TNF- α activate pro- and anti-apoptotic gene expression programs mediated by late nuclear localization of NF-κB, whereas low-dose TNF- α signals do not lead to apoptosis-related signalling due to a lack of late-term nuclear localization. Furthermore, other signalling molecules and regulatory proteins are also upregulated at early times, including *Il6*, *Ccl20*, *Icam1* and *Zfp36*, suggesting possible synergistic or interfering mechanisms.

The wealth of biochemical data has resulted in a number of mathematical models that describe TNF- α -induced NF-κB nuclear oscillations. Some models are deterministic and therefore unable to reproduce the heterogeneity in single cells^{12,17}. Later models incorporate negative regulation of NF-κB by A20^{22,23}, and use a stochastic description of slow dynamics^{24,25}. These models are able to explain the response of the network to repeating short pulses of TNF- α in SK-N-AS cells¹³. Digital cell activation and the overall response characteristics we observed are not simultaneously present in any previous model. We therefore revised the stochastic model²⁵ to account for our observations. First, we considered the effects of limited TNF- α amount present in the microfluidic chambers and TNF- α degradation on overall TNF- α loss, and included cellular variation in the amount of TNF- α receptor (see Supplementary Mathematical Methods). The resulting model, although more realistic, did not produce the digital activation that we observed at low doses. We therefore implemented a nonlinear IKK (inhibitor of NF-κB kinase) activation profile, where the activation rate of IKK depends quadratically on the concentration of the upstream kinase IKKK. Such a nonlinear activation rate may be justified by the fact that IKK subunits IKK- α and IKK- β must be phosphorylated at two

serine residues, S177 and S181, to attain full activity²⁶. Incorporation of the quadratic activation resulted in achieving the digital cellular response simulations similar to our experiments (Fig. 3).

The model (Fig. 3a) was manually fitted to the single-cell traces, and a single set of biochemically measured, assumed and fitted parameters were used for all the simulations (see Supplementary Mathematical Methods for model fitting). The core model comprises 16 ordinary differential equations representing biochemical reactions and 34 rate constants, where 20 of the constants are fixed (biochemically measured or based on related data), and the other 14 were varied for model fitting within biologically reasonable boundaries. The internal parameters of the model, such as the number of proteins and mRNAs, production, degradation and transport rates, are all biologically plausible values.

The simulated single-cell traces for 3T3 cells at different TNF- α doses can be seen in Fig. 3c, d and Supplementary Fig. 11, which agree well with the data in terms of timing, intensity and the variability of the first peaks at all doses. Most remarkably, the model can reproduce—within a single set of biochemical parameters—the measured concentration-dependent single-cell activation probability (Fig. 3b), mean nuclear NF-κB intensities (Fig. 3e), the response times (Fig. 3f), and their distributions. Furthermore, it predicts with excellent accuracy the fraction of cells responding to consecutive short pulses of low-dose TNF- α (Fig. 4a). Although the model captures many features of our single-cell microscopy data, it falls short of perfectly reproducing the total number of oscillations at mid doses (Supplementary Fig. 11), first peak decay times and peak-to-peak intensity ratios shown in Supplementary Figs 4–7. Simulated expression profiles for early, intermediate and late genes can be seen in Fig. 4b. The gene expression closely follows NF-κB dynamics and agrees well with most of the genes we measured in Fig. 2. Some measured expression profiles such as *Trail* and *Ccl2* do not follow NF-κB nuclear localization strictly and the single transcription factor model we used was not able to reproduce these profiles, which indicates that parallel synergistic or interfering pathways significantly contribute to transcription of these genes²⁷.

We have mapped the nuclear localization dynamics of NF-κB under TNF- α stimulation by measuring thousands of single-cell traces and

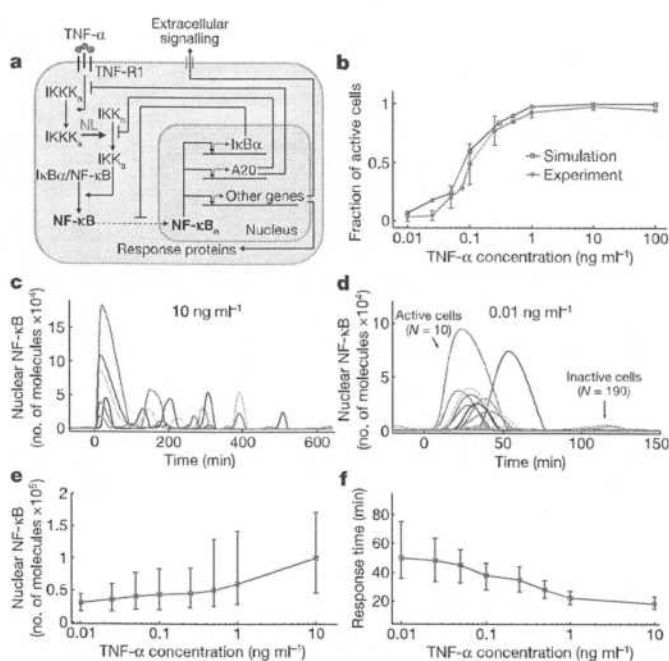


Figure 3 | Mathematical model development and simulations. Where applicable, error bars show standard deviation from the mean. **a**, Model architecture is based on stochastic description of receptor and gene activity, quadratic representation of IKK activation, and negative feedback via I κ B α . **b**, Simulated (blue) and measured (red) fraction of activated cells. **c, d**, Simulated single-cell NF- κ B nuclear localization traces at the experimentally measured TNF- α concentration range. The low dose (0.01 ng ml^{-1}) stimulated cells show clear separation between active and non-active cells similar to experiments. Among 200 simulated cells, only 10 were activated. The model faithfully reproduces important aspects of experimental means and distributions (shown with error bars) across all concentrations. **e**, Simulated NF- κ B nuclear intensity versus TNF- α concentration (see Fig. 1h). **f**, Simulated NF- κ B response time versus TNF- α concentration (see Fig. 1i).

time-dependent gene expression profiles over a concentration range of four orders of magnitude. A mathematical model that reproduces NF- κ B dynamics and transcription at the measured concentration range was developed, constituting a significantly improved model of the NF- κ B pathway under TNF- α stimulation. We have found that cells activate in response to TNF- α in a digital manner. Although the fraction of activated cells decreases to zero with decreasing TNF- α dose, the NF- κ B amplitude remains high, allowing high expression of early genes. Early gene expression is not dependent on the inducing signal intensity, whereas the expression of later genes requires persistent nuclear localizations of the transcription factor, which exist only at the highest input signal levels. The cells process analogue signal intensity information using a diverse set of parameters such as the timing, peak intensity and number of transcription factor oscillations to create digital outputs (activation and early gene expression). In addition to their biological significance, our findings highlight the importance of high-quality, single-cell data in understanding and modelling biological systems, and demonstrate the efficiency of high-throughput microfluidic techniques in obtaining such data.

METHODS SUMMARY

We used a lentiviral system to create *p65*^{-/-} mouse fibroblast (3T3) cells expressing the fluorescent fusion protein p65-DsRed under control of the endogenous mouse *p65* promoter⁸. To relieve a bottleneck in image processing in this study, we also infected the cells with a lentivirus containing the nuclear marker H2B-GFP driven by the human ubiquitin C promoter. Various TNF- α (Roche) dilutions in DMEM were kept on ice at all times and these fluids were flowed into the microfluidic chambers during stimulation. Once the TNF- α media was flowed in, the chambers were sealed and were imaged every 6 min in both GFP and DsRed fluorescence channels, for up to 12 h. For gene expression measurements, we used

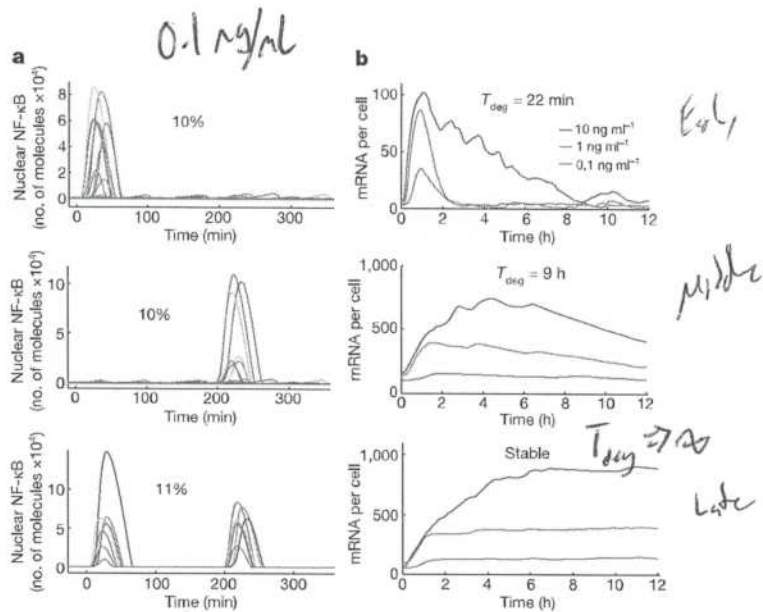


Figure 4 | Model predictions: stochastic and variable cell switching and target gene expression dynamics. **a**, Simulated single-cell traces for low-dose, short-pulsed stimulation. Cells were stimulated with two consecutive 20-min-long pulses of 0.1 ng ml^{-1} TNF- α . The pulses were separated by 180 min. Ten per cent respond to only the first pulse (top), 10% respond only to the second pulse (middle) and 11% of the cells in the chamber respond to both pulses (bottom), showing excellent agreement with experimental results shown in Fig. 1j–l. **b**, Simulations of early (top), intermediate (middle) and late (bottom) term NF- κ B target genes under various doses of TNF- α . The model reproduces basic features of the expression profiles shown in Fig. 2a by varying only the transcript degradation times (T_{deg}).

cells cultured in well plates that were stimulated with different TNF- α concentrations. At the end of each stimulation experiment (0.25, 0.5, 2, 4, 6, 8, 10 and 12 h after stimulation), cells were lysed and cDNA was synthesized using Cell Direct One Step RT-PCR kit (Invitrogen). TaqMan primers and probes (Applied Biosystems) were used for real-time qPCR (Fluidigm 48x48 Dynamic Array). The relative gene expression levels were then calibrated for total mRNA molecules per cell via digital-PCR measurements¹⁰ (Fluidigm 12 Digital PCR Chip). In Fig. 2b, c, we estimate the mRNA levels for only active cells by dividing the expression levels by the fraction of active cells at each dose measured in Fig. 1b.

Full Methods and any associated references are available in the online version of the paper at www.nature.com/nature.

Received 29 December 2009; accepted 28 April 2010.

Published online 27 June 2010.

1. Hayden, M. S., West, A. P. & Ghosh, S. NF- κ B and the immune response. *Oncogene* **25**, 6758–6780 (2006).
2. Cheong, R. et al. Transient I κ B kinase activity mediates temporal NF- κ B dynamics in response to a wide range of tumor necrosis factor- α doses. *J. Biol. Chem.* **281**, 2945–2950 (2006).
3. Gómez-Sjöberg, R., Leyrat, A. A., Pirone, D. M., Chen, C. S. & Quake, S. R. Versatile, fully automated, microfluidic cell culture system. *Anal. Chem.* **79**, 8557–8563 (2007).
4. Batchelor, E., Loewer, A. & Lahav, G. The ups and downs of p53: understanding protein dynamics in single cells. *Nature Rev. Cancer* **9**, 371–377 (2009).
5. Spencer, S. L., Gaudet, S., Albeck, J. G., Burke, J. M. & Sorger, P. K. Non-genetic origins of cell-to-cell variability in TRAIL-induced apoptosis. *Nature* **459**, 428–432 (2009).
6. Lahav, G. et al. Dynamics of the p53-mdm2 feedback loop in individual cells. *Nature Genet.* **36**, 147–150 (2004).
7. Covert, M. W., Leung, T. H., Gaston, J. E. & Baltimore, D. Achieving stability of lipopolysaccharide-induced NF- κ B activation. *Science* **309**, 1854–1857 (2005).
8. Lee, T. K. et al. A noisy paracrine signal determines the cellular NF- κ B response to LPS. *Sci. Signal.* **2**, 93 (2009).
9. Cohen, A. A. et al. Dynamic proteomics of individual cancer cells in response to a drug. *Science* **322**, 1511–1516 (2008).
10. Hoffmann, A. & Baltimore, D. Circuitry of nuclear factor κ B signalling. *Immunol. Rev.* **210**, 171–186 (2006).
11. Courtois, G. & Gilmore, T. D. Mutations in the NF- κ B signalling pathway: implications for human disease. *Oncogene* **25**, 6831–6843 (2006).

12. Nelson, D. E. et al. Oscillations in NF- κ B signaling control the dynamics of gene expression. *Science* **306**, 704–708 (2004).
13. Ashall, L. et al. Pulsatile stimulation determines timing and specificity of NF- κ B-dependent transcription. *Science* **324**, 242–246 (2009).
14. St. Pierre, F. & Endy, D. Determination of cell-fate selection during phage lambda infection. *Proc. Natl Acad. Sci. USA* **105**, 20705–20710 (2008).
15. Snijder, B. et al. Population context determines cell-to-cell variability in endocytosis and virus infection. *Nature* **461**, 520–523 (2009).
16. Elowitz, M., Levine, A. J., Siggia, E. D. & Swain, P. S. Stochastic gene expression in a single cell. *Science* **297**, 1183–1186 (2002).
17. Hoffmann, A., Levchenko, A., Scott, M. L. & Baltimore, D. The I κ B-NF- κ B signaling module: temporal control and selective gene activation. *Science* **298**, 1241–1245 (2002).
18. Hao, S. & Baltimore, D. The stability of mRNA influences the temporal order of the induction of genes encoding inflammatory molecules. *Nature Immunol.* **10**, 281–288 (2009).
19. Giorgetti, L. et al. Noncooperative interactions between transcription factors and clustered DNA binding sites enable graded transcriptional responses to environmental inputs. *Mol. Cell* **37**, 418–428 (2010).
20. Bhat, S., Hermann, J., Armishaw, P., Corbisier, P. & Emslie, K. R. Single molecule detection in nanofluidic digital array allows accurate measurement of DNA copy number. *Anal. Bioanal. Chem.* **394**, 457–467 (2009).
21. Wilson, J. W., Catherine, B. & Christopher, S. (eds) in *Apoptosis Genes* (Springer, 1999).
22. Lee, E. G. et al. Failure to regulate TNF- α -induced NF- κ B and cell death responses in A20-deficient mice. *Science* **289**, 2350–2354 (2000).
23. Hutt, J. E. et al. I κ B kinase beta phosphorylates the K63 deubiquitinase A20 to cause feedback inhibition of the NF- κ B pathway. *Mol. Cell. Biol.* **27**, 7451–7461 (2007).
24. Lipniacki, T., Paszek, P., Brasier, A. R., Luxon, B. & Kimmel, M. Mathematical model of NF- κ B regulatory module. *J. Theor. Biol.* **228**, 195–215 (2004).
25. Lipniacki, T., Puszynski, K., Paszek, P., Brasier, A. R. & Kimmel, M. Single TNF- α trimers mediating NF- κ B activation: Stochastic robustness of NF- κ B signaling. *BMC Bioinformatics* **8**, 376 (2007).
26. Delhaise, M., Hayakawa, M., Chen, Y. & Karin, M. Positive and negative regulation of I κ B kinase activity through IKK subunit phosphorylation. *Science* **284**, 309–313 (1998).
27. Chen, Y.-M. et al. Dual regulation of TNF- α induced CCL2/monocyte chemoattractant protein-1 expression in vascular smooth muscle cells by NF- κ B and AP-1: modulation by type III phosphodiesterase inhibition. *J. Pharmacol. Exp. Ther.* **103**, 06262 (2004).
28. Toepke, M. W. & Beebe, D. J. PDMS absorption of small molecules and consequences in microfluidic applications. *Lab Chip* **6**, 1484–1486 (2006).

Supplementary Information is linked to the online version of the paper at www.nature.com/nature.

Acknowledgements We thank A. Leyrat and R. Gomez-Sjöberg for development of the automated cell culture system, assistance with the software, and for contributions to experimental design and preliminary data. This research was supported in part by an NIH Director's Pioneer Award (to S.R.Q.), an NCI Pathway to Independence Award (K99CA125994) (to M.W.C.), the Foundation for Polish Science (TEAM 2009-3/6) and NSF/NIH grant no. R01-GM086885 (to T.L.), a Stanford Graduate Fellowship (to T.K.L.), and a Stanford Bio-X Graduate Fellowship (to J.J.H.).

Author Contributions S.T. and J.J.H. performed the experiments, S.T. and T.L. developed the mathematical models and performed the simulations, T.K.L. developed the image processing methods and all authors contributed to analysis of the data and to writing the manuscript.

Author Information Reprints and permissions information is available at www.nature.com/reprints. The authors declare competing financial interests: details accompany the full-text HTML version of the paper at www.nature.com/nature. Readers are welcome to comment on the online version of this article at www.nature.com/nature. Correspondence and requests for materials should be addressed to M.W.C. (mcovert@stanford.edu), S.R.Q. (quake@stanford.edu) or T.L. (tlipn@ippt.gov.pl).

METHODS

Cell lines. We previously used a lentiviral system to create $p65^{-/-}$ mouse fibroblast (3T3) cells expressing the fluorescent fusion protein p65–DsRed under control of the endogenous mouse $p65$ promoter⁸. Overexpression of p65 can cause unusual NF-κB activation, and we therefore cloned the 1.5 kb upstream of the *relA* gene into the lentiviral construct to control p65–DsRed expression. We used the resulting construct to infect $p65^{-/-}$ 3T3 cells (courtesy of the D. Baltimore laboratory). These cells showed a normal response to TNF- α at the population level⁹. To relieve a bottleneck in image processing in this study, we also infected the cells with a lentivirus containing the nuclear marker H2B–GFP driven by the human ubiquitin C promoter. After cloning, the cells were frozen and newly thawed cells were used for each experiment to prevent 3T3 cell re-transformation and to minimize heterogeneity. A correlation between p65–DsRed levels and cell activation was not observed⁹.

Microfluidic cell culture experiments. Cells were seeded at constant density around 20,000 cells cm^{-2} (200 ± 25 cells per chamber) into microfluidic chambers and were cultured for one day to reach near 50% confluence before stimulation experiments. The external conditions were set to standard culture conditions (5% CO_2 and 37 °C external temperature) and maintained at this level. During cell growth, 33% of the chamber volume was replaced with fresh media (DMEM) every hour using the nanolitre microfluidic pump, which resulted in vigorous proliferation of 3T3 cells. We made sure that cells were healthy, motile and proliferating before TNF- α stimulation experiments. We were able to establish such cultures for durations up to a week in the microfluidic chambers, depending on initial seeding density. During stimulation experiments, various TNF- α (Roche) dilutions in DMEM were kept on ice at all times and the fluids were flowed quickly into the microfluidic chambers during stimulation to avoid degradation of TNF- α . The high surface-area to volume ratio of the plastic tubing and the microfluidic environment we used allow rapid warming of the media when it enters the environmental chamber, therefore the media flown in the chambers were at ambient (37 °C) temperature. The media and TNF- α vials were pressurized with 5% CO_2 to minimize pH change. Cell viability was not affected negatively during media flow and stimulation. The microfluidic culture chip⁹ allows the replacement of the entire culture media in less than a second, which results in a step-like TNF- α concentration profile on the timescales of NF-κB dynamics. Once the TNF- α loaded media was flowed in, the chambers were sealed and were imaged every 6 min in both GFP and dsRed fluorescence channels during the entire experiment, for up to 12 h. The cells were not fed with media after stimulation and during imaging; they remained in the same TNF- α loaded media during the entire experiment without disturbance. All TNF- α concentrations (up to ten at a time) were tested in parallel chambers (with duplicates) in a single experiment, and such experiments were repeated multiple times with minimal variation between results. We therefore tested up to 20 different microfluidic chambers at a time. We have not observed any negative effect due to TNF- α adsorption into PDMS-based microfluidics, although absorption into PDMS needs to be taken into account when small, hydrophobic molecules are used²⁸.

Image acquisition and quantification. Cells were imaged in both the GFP and DsRed channels with a Leica DMI6000B microscope (20× air objective) and Retiga-SRV CCD camera (Q Imaging) every 5–6 min for several hours. Cell traces were visually checked and compared to images to exclude mitotic cells, as mitotic cells typically show increased signal intensity that could be confused with active cells. The fraction of responding cells at each concentration was calculated as the number of responding cells divided by the sum of responding and non-responding cells. To generate time courses of NF-κB localization in single cells, custom Matlab software using the Image Processing Toolbox was used to automatically identify the nuclei from H2B–GFP images and extract nuclear intensities from p65–DsRed images. To identify nuclear regions, H2B–GFP images were local range contrast filtered with a neighbourhood of three pixels and then thresholded, where the threshold level was automatically determined by k -means clustering pixel intensities

with $k = 3$. Touching or merged nuclei (determined by solidity <0.925) were then separated by a watershed transform with markers seeded at k -means clustered centroids. Nuclei between time points were then linked to the nearest nuclei in the next time point and preliminary quality control checked for constant nuclear area through tracking. H2B–GFP and p65–DsRed images were aligned by cross-correlation when necessary and nuclear intensities were then extracted from the associated p65–DsRed image. For the first time point, cytoplasmic areas and p65–DsRed intensities were extracted through a combination of local thresholding and watershed transforms with the nuclei as marker seeds. All cell tracking was manually checked to eliminate mistakes by the automated analysis. Cells that divided or left the field of view during the experiment were not included in the analysis of NF-κB localization dynamics. Time courses of NF-κB localization were linked to the responding or non-responding classification using the XY coordinates in the field of view. The mspeaks function in the Bioinformatics Toolbox of Matlab was used to identify peaks in NF-κB nuclear localization and to calculate the times of full-width half maximum of the first peak. Localization dynamics from cells that were judged to be non-responders were used to determine a peak threshold for responding cells. Because we could not always image the ascending portion of the first peak with sufficient temporal resolution, we calculated the difference between the time of the first peak (response time) and the later full-width half maximum time, which we called the first peak decay time. Subsequent statistical analysis was performed with Matlab.

Nuclear localization peak intensity, timing and area. The peak intensity and timings of the peaks were found using custom peak detection software written in Matlab. The area under each nuclear localization peak is a measure of the total NF-κB nuclear activity that lead to the transcription of target genes (that is, the total amount and duration of NF-κB presence in the nucleus), whereas the peak intensity is a measure of the maximum level of the transcriptional activity. At each dose, the area of the first peak was integrated from the time of TNF- α stimulation to the first minimum for each cell using Matlab. The delayed rise time observed during low-dose stimulation results in increased peak width, which compensates the reduced peak intensity, resulting in nearly equal mean first-peak areas at all doses.

Gene expression measurements. Cells cultured in well plates were stimulated with six different TNF- α concentrations from 0.01 ng ml^{-1} to 10 ng ml^{-1} prepared in DMEM media. At the end of each stimulation experiment (0.25, 0.5, 2, 4, 6, 8, 10 and 12 h after stimulation), cells were lysed and cDNA was synthesized using Cells Direct One Step RT–PCR kit (Invitrogen), and TaqMan primers and probes (Applied Biosystems) were used for real-time qPCR. These were population-based measurements, with nearly 500 cells in each qPCR reaction, containing both active and non-active cells. Each experimental condition had quadruplicate replicates, and was compared to control wells where cells were not stimulated with TNF- α . Each condition was measured at least three times. We used microfluidic dynamic arrays (Fluidigm 48x48 Dynamic Array) to perform 2,304 qPCR reactions in parallel, and all 64 × 24 experiments ($\times 4$ replicates of each reaction) consumed three dynamic arrays. The cycle thresholds (C_T) (Supplementary Table 2) measured during qPCR reactions were converted into relative expression levels (2^{-C_T}). The relative gene expression levels were then calibrated for total mRNA molecules per cell via digital-PCR measurements performed on a single gene (Fluidigm 12 Digital PCR Chip)²⁹. Figure 2a shows mRNA levels measured on populations that contain active and non-active cells, and includes the baseline (no TNF- α) level expression. In Fig. 2b, c, we estimate the mRNA levels for only active cells, by first subtracting the baseline level, and then dividing the differential expression levels with the fraction of active cells at each dose measured in Fig. 1, and finally calibrating using digital-PCR measurements. Figure 2b shows that early genes are expressed at very high levels in active cells even at the lowest TNF- α doses, demonstrating how single-cell data can be used to interpret population-based measurements of gene expression.

SUPPLEMENTARY INFORMATION

Supplementary Mathematical Methods

The mathematical analysis of the NF- κ B pathway regulation is discussed in two sections. First, we consider TNF α -TNFR1 interactions in the microfluidic chamber. Next, in a separate single-cell stochastic model, we analyze dynamics of NF- κ B controlled by interlinked negative feedback loops mediated by A20 and I κ B α .

1.TNF α -TNFR1 kinetics

The kinetics of TNF α molecules in the experimental chamber involves four processes:

- 1) TNF α degradation
- 2) TNF α -TNFR1 association
- 3) TNF α -TNFR1 dissociation
- 4) Internalization of TNFR1

In addition to binding dissociation, diffusion and internalization rates, these processes are further controlled by the two parameters specific for the experimental apparatus used and conditions tested: (1) chamber volume per cell and (2) the initial TNF α concentration. The chamber volume - which is often omitted when calculating receptor dynamics - is of key importance especially at low volumes since it determines the available number of TNF α (trimers) molecules per cell. It is especially important at low doses when this number is smaller than number of TNF α receptors available for binding (thousands per cell). In the 35 nanoliter microfluidic chambers we used, the effective loss of free TNF α is due to natural degradation (half life~1h) and to binding to TNF α receptors, which are then internalized. According to Grell et al. (1998), the TNF α -TNFR1 dissociation half-time (33 min) is about twice longer than the internalization half-time (10-20 min), as a result bound TNF α molecules are mostly internalized than dissociate. At low TNF α doses the internalization mechanism becomes more effective than natural degradation and the effective loss of free TNF α in our experimental conditions is much faster than degradation (Fig. M1). The effective free TNF α loss rates in our microfluidic chambers are estimated as $2 \times 10^{-4} \text{ s}^{-1}$, $7 \times 10^{-4} \text{ s}^{-1}$, $7.7 \times 10^{-4} \text{ s}^{-1}$ and $8.3 \times 10^{-4} \text{ s}^{-1}$ for 10ng/ml, 1ng/ml, 0.1ng/ml, and 0.01ng/ml TNF α concentrations, respectively. These rates were used in main model for simulations of cell activation and response dynamics in the microfluidic chamber.

$\approx 75\%$
Internalization

For experimental chambers with larger volume, the peak numbers of bound TNF α -TNFR1 ligand-receptor complexes are similar to those in lower volumes (Figure M.2). However, at larger volumes significantly higher level of bound complexes are maintained after the peak, which should lead to prolonged activity of TNF α induced NF- κ B (i.e. larger fraction of active cells, late activating cells) in such volumes. The parameters used in these calculations can be seen in Table 1.

Table 1. Parameters for TNF α -TNFR1 kinetics.

symbol	value	Reaction and reference
k_{on}	$1.83 \times 10^7 \text{ M}^{-1} \text{ s}^{-1}$	$\text{TNF} + \text{TNFR1} \rightarrow \text{TNF TNFR1}$ Grell et al. (1998)
k_{off}	$3.48 \times 10^{-4} \text{ s}^{-1}$	$\text{TNF TNFR1} \rightarrow \text{TNF} + \text{TNFR1}$ Grell et al. (1998)
k_{int}	$7.70 \times 10^{-4} \text{ s}^{-1}$	$\text{TNF TNFR1} \rightarrow \text{TNF TNFR1}_{int}$ Grell et al. (1998)
c_{deg}	$2 \times 10^{-4} \text{ s}^{-1}$	$\text{TNF} \rightarrow \emptyset$ this study

The equations describing receptor dynamics are:

Free TNF α

$$\frac{d}{dt} \text{TNF}(t) = -k_{on} \times \text{TNF}(t) \times \text{TNFR1}(t) - c_{deg} \times \text{TNF}(t) + k_{off} \times (\text{TNF|TNFR1})(t)$$

Free TNFR1 receptors

$$\frac{d}{dt} \text{TNFR1}(t) = -k_{on} \times \text{TNF}(t) \times \text{TNFR1}(t) + (c_{deg} + k_{off}) \times (\text{TNF|TNFR1})(t)$$

*Agnant TNF α binds on the
receptor complex*

TNFR1-TNF α complexes

$$\frac{d}{dt} (\text{TNF|TNFR1})(t) = k_{on} \times \text{TNF}(t) \times \text{TNFR1}(t) - (c_{deg} + k_{off} + k_{int}) \times (\text{TNF|TNFR1})(t)$$

“The first time I saw you, I was so taken by your beauty and intelligence that I fell in love with you immediately. You are the most wonderful person I have ever met, and I would do anything for you. I know that we are from different backgrounds, but I believe that our love is strong enough to overcome any obstacle. I want to spend the rest of my life with you, and I hope you will consider my proposal.”



“I am honored to accept your proposal, and I thank you for your kind words and thoughtful gesture.”

“I am so happy that you accepted my proposal. We will start planning our wedding right away.”

“I am looking forward to our future together and to the many adventures we will have as a couple.”

“I am so happy that you accepted my proposal. We will start planning our wedding right away.”

“I am looking forward to our future together and to the many adventures we will have as a couple.”

“I am so happy that you accepted my proposal. We will start planning our wedding right away.”

“I am looking forward to our future together and to the many adventures we will have as a couple.”

“I am so happy that you accepted my proposal. We will start planning our wedding right away.”

“I am looking forward to our future together and to the many adventures we will have as a couple.”

TNFR1-TNF α complexes internalized

$$\frac{d}{dt}(\text{TNF} | \text{TNFR1})_{\text{int}}(t) = k_{\text{int}} \times (\text{TNF} | \text{TNFR1})(t)$$

Binding of the TNF α to TNFR1 does not necessarily lead to formation of the active TNF α receptor complexes that lead to NF- κ B pathway activation. First, the downstream signaling requires TNFR1 trimerization, which may take place before TNF α trimer binding (see Chan 2007 for discussion). Next, the adapter protein TRADD binds and serves as an assembly platform for TRAF2 and RIP. At this step the IKKK (IKK kinase) maybe activated, alternatively TRADD and RIP associate with FADD and cell-death-initiation caspase 8 (complex II), which then activates executioner caspase 3 leading to apoptic DNA fragmentation. As a result one can expect that the number of complexes that serve as IKKK activation platform is smaller than the number of bound TNF α trimer molecules.

2. NF- κ B pathway regulation in the single cell

The current model follows our previous model (Lipniacki et al. 2007) that involved two-compartment kinetics of NF- κ B and its inhibitors A20 and I κ B α , and allowed for analysis of single cell responses to TNF α stimulation of arbitrary and time dependent intensity, in both wild type and A20 deficient cells. The model combines the two feedback NF- κ B-I κ B α -A20 regulatory module with the signal transduction-amplification cascade, which transmits the signal from the TNFR1 receptors.

Receptor activation and signal transduction pathway

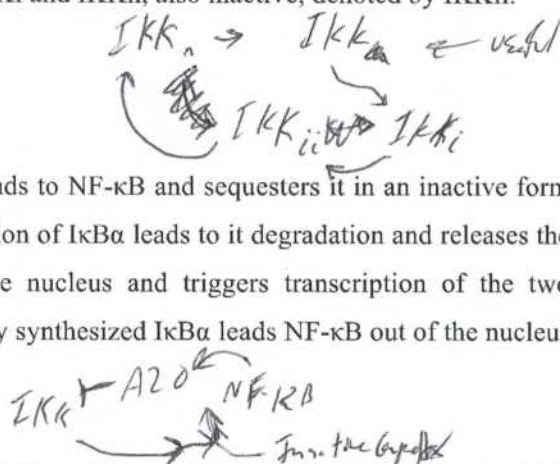
The single event of receptor activation is amplified by the three-step signal transduction cascade involving activation of kinases named IKKK (IKK activating kinase) and IKK. Biologically, there are at least two kinases involved in this process: MEKK3 and TAK1. We assume that IKKK migrates toward the receptor and is activated at the receptor (transformation from IKKKn to IKKKa). Active IKKKa molecules activate IKK molecules (transformation from IKKn to IKKa). Since full activation of IKK requires its phosphorylation at two serine residues Ser177 and Ser181 (Delhase et al., 1999), we assume in this model that IKK activation rate is proportional to square of active IKKKa. In turn active IKKa phosphorylate I κ B α molecules leading to their

M.49
Actm R.J.W.
Lmbel

ubiquitination and degradation. It is assumed that the total number of IKKK and IKK molecules (as well as of the NF- κ B molecules) is constant; i.e., their degradation is balanced by production, but both terms are omitted in the mathematical representation. The IKKK may exist in one of two states: native neutral IKKKn, specific to unstimulated resting cells; and active IKKKa. IKK complexes, consisting of catalytic subunits IKK α and IKK β and regulatory subunits IKK γ , may exist in one of four states: native neutral (denoted by IKKn), specific to unstimulated resting cells; active (denoted by IKKa) arising from IKKn via phosphorylation of serines 177 and 181 of IKK subunits (Delhase et al., 1999) upon the IKKKa induced activation; inactive (denoted by IKKi) but different from the native neutral form, arising from IKKa possibly due to overphosphorylation; and transient between IKKi and IKKn, also inactive, denoted by IKKii.

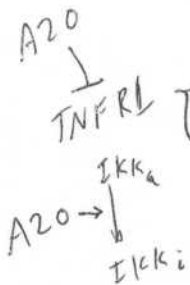
The NF- κ B-I κ B α -A20 regulatory module

In resting cells, the unphosphorylated I κ B α binds to NF- κ B and sequesters it in an inactive form in the cytoplasm. IKKa mediated phosphorylation of I κ B α leads to its degradation and releases the main activator NF- κ B, which then enters the nucleus and triggers transcription of the two inhibitors and numerous other genes. The newly synthesized I κ B α leads NF- κ B out of the nucleus and sequesters it in the cytoplasm.



I κ B α /NF- κ B
 In the cytoplasm

IKK inactivation is controlled by the second inhibitor A20, which is strongly up-regulated by NF- κ B (Krikos et al., 1992). The exact mechanism of A20 action is still not fully resolved. Here, we assume that A20 acts in two ways: (1) It initiates degradation of RIP, the key component of the TNFR1 receptor complex (Wertz et al., 2004), which attenuates the activity of receptors, and (2) it directly associates with IKK (Zhang et al., 2000) enhancing IKKa conversion to catalytically inactive form IKKi (the conversion from IKKa to IKKi takes place also in A20 deficient cells but at a slower rate). The exact mechanism of IKK inactivation also remains unresolved: According to Delhase et al., (1999) IKK inactivates via autophosphorylation of serines in IKK C-terminal region. However, Schomer-Miller et al. (2006) found that this autophosphorylation does not diminish IKK activity and suggested that phosphorylation of serines 740 and 750 in NBD/BD domain of IKK may have a regulatory role and that their phosphorylation may downregulate IKK activity. The form IKKi spontaneously converts into IKKn through several inactive intermediate forms collectively denoted by IKKii. The number of these forms may be large since there are at least 16 serine residues in IKK, which may be involved in regulation of IKK activity according to Schomer-Miller et al. (2006). This intermediate step is introduced in our model to account for the



the period 1970–1975, which had not yet ended at the time of the study. This was due to the fact that the period 1970–1975 was considered to be the most difficult period in the history of the country, and the period 1976–1980 was considered to be the most favourable period. In 1970–1975, the economy was in a state of stagnation, and there was a sharp increase in inflation. In 1976–1980, the economy was in a state of recovery, and there was a sharp decrease in inflation. The period 1970–1975 was characterized by a sharp increase in the cost of living, and the period 1976–1980 was characterized by a sharp decrease in the cost of living. The period 1970–1975 was characterized by a sharp increase in the cost of living, and the period 1976–1980 was characterized by a sharp decrease in the cost of living.

Methodology and design of the study

The methodology used in this study is the descriptive-analytical method. The main purpose of this study is to describe the economic situation in the country during the period 1970–1975 and 1976–1980, and to analyze the causes of the economic situation in the country during the period 1970–1975 and 1976–1980. The main purpose of this study is to describe the economic situation in the country during the period 1970–1975 and 1976–1980, and to analyze the causes of the economic situation in the country during the period 1970–1975 and 1976–1980.

The study was conducted in two stages. The first stage was the collection of primary data, which was carried out through interviews with experts in the field of economics and statistics. The second stage was the analysis of the collected data, which was carried out through statistical methods. The data collected in the first stage were used to identify the main trends in the economy during the period 1970–1975 and 1976–1980. The data collected in the second stage were used to identify the causes of the economic situation in the country during the period 1970–1975 and 1976–1980. The data collected in the first stage were used to identify the main trends in the economy during the period 1970–1975 and 1976–1980. The data collected in the second stage were used to identify the causes of the economic situation in the country during the period 1970–1975 and 1976–1980.

*N Time Step
N Time Delay*

delay needed to process the inactivated form IKKi into native state IKKn. This effect is manifested in A20^{-/-} cells under persistent or long lasting TNF α stimulation as a down-regulation of IKK activity at about 30 minutes followed by a higher plateau. According to our model in the first minutes of high dose TNF α stimulation most of IKKn is used up so the IKK activation rate is low. The activation rate and the level of IKKa may increase only after some IKKn is recovered via the intermediate form IKKii.

Recently, White and colleagues proposed that A20 does not act between IKKa and IKKi, but slows down the restoration of IKKn from inactive form IKKi (Ashall et al. 2009). Such assumption allows for reproduction of the system responses to pulse-pulse-pulse stimulation in a very broad range (4 orders of magnitude) of A20 degradation parameters. However, after such a modification, we encounter difficulties in reproducing the kinetics of A20^{-/-} cells. Our current model, after adjusting the parameters, properly reproduces short pulse experiments by Ashall et al. (2009).

*IKKi
↓ A20
IKKa*

The inhibitor I κ B α migrates between the nucleus and cytoplasm and forms complexes with NF- κ B molecules. The nuclear I κ B α -NF- κ B complexes quickly migrate into the cytoplasm. The second inhibitory protein A20 is considered only in the cytoplasm where it triggers the inactivation of IKK. It is assumed that the transformation rate from IKKa into IKKi is the sum of the constant term and a term proportional to the amount of A20. The transcriptional regulation of

*b + pA20
Is (...) IKK α ?*

b A20 and I κ B α genes is governed by the same rapid elongation regulatory mechanism with a rapid coupling between NF- κ B binding and transcription. The mechanisms for NF- κ B dependent regulation of I κ B α and A20 are based on the control of transcriptional elongation. In this situation, stalled RNA polymerase II is rapidly activated by NF- κ B binding to enter a functional elongation mode, and requires continued NF- κ B binding for re-initiation. This is represented in our model by tight coupling of NF- κ B binding to mRNA transcription. We assume that all cells are diploid, and both A20 and I κ B α genes have two potentially active homologous copies, each of which is independently activated due to binding of NF- κ B molecule to a specific regulatory site in gene promoter. Following our previous studies (Lipniacki et al. 2006 and 2007) we made the simplifying assumption that each gene copy may exist only in one of two states; active and inactive. When the copy is active the transcription is initiated at a high rate, when the copy is inactive transcription is inhibited. The gene copy becomes inactive when the NF- κ B molecule is removed from its regulatory site due to the action of I κ B α molecules, which bind to DNA-associated NF- κ B, exporting it out of the nucleus.

*Yes
(3, 4)*

*Transcrip^{fm} Elong^{fm}
Build^{fm} RNA by
pol.*

Sources of heterogeneity in NF-κB regulation

We consider two types of molecular noise sources in this model:

1. Extrinsic noise: due to different levels of total NF-κB and TNFR-1 across the population. Our experiments show heterogeneity in total cell fluorescence, indicating that RelA levels in individual cells are not equal. Furthermore, many cell types including 3T3's we used have considerable variation in their TNFR-1 levels, which leads to variable sensitivity to TNF α . Accordingly, we assume in our model that total NF-κB and TNFR-1 follow the log normal distributions defined as

$$f = \frac{A}{x\sigma\sqrt{2\pi}} \text{Exp}\left(-\frac{(\ln(x) - \mu)^2}{2\sigma^2}\right) \quad x > 0$$

with

$$\text{mean} = A \times \text{Exp}(\mu + \sigma^2/2), \text{ median} = A \times \text{Exp}(\mu), \text{Var} = (\text{Exp}(\sigma^2) - 1)\text{Exp}(2\mu + \sigma^2)$$

For NF-κB we assume: $A_N = 10^5$, $\sigma_N = 1/\sqrt{2}$, $\mu_N = -1/4$

$\sigma^2 = \frac{\sigma^2}{l}$

$$\text{mean}_N = A_N, \text{ median}_N = A_N \times e^{-1/4}, \quad \text{Var}_N = A_N^2 \times (e^{1/2} - 1)$$

and for TNFR-1 receptors:

$$A_R = 2 \times 10^3, \quad \sigma_R = \sqrt{2}, \quad \mu_R = -1$$

$$\text{mean}_R = A_R, \quad \text{median}_R = A_R \times e^{-1}, \quad \text{Var}_R = A_R^2 \times (e^2 - 1)$$

2. Intrinsic noise: resulting from discrete regulation of receptor activity (ligand-receptor binding, trimerization and recruitment of adaptor proteins) and transcription of A20, IκBa, TNF α and reporter genes (gene- NF-κB binding), as in Lipniacki et al. (2007).

the first time in history that the U.S. has been able to do this without having to pay for it.

It's also the first time in history that the U.S. has been able to do this without having to pay for it.

It's also the first time in history that the U.S. has been able to do this without having to pay for it.

It's also the first time in history that the U.S. has been able to do this without having to pay for it.

It's also the first time in history that the U.S. has been able to do this without having to pay for it.

It's also the first time in history that the U.S. has been able to do this without having to pay for it.

It's also the first time in history that the U.S. has been able to do this without having to pay for it.

It's also the first time in history that the U.S. has been able to do this without having to pay for it.

It's also the first time in history that the U.S. has been able to do this without having to pay for it.

It's also the first time in history that the U.S. has been able to do this without having to pay for it.

It's also the first time in history that the U.S. has been able to do this without having to pay for it.

It's also the first time in history that the U.S. has been able to do this without having to pay for it.

It's also the first time in history that the U.S. has been able to do this without having to pay for it.

It's also the first time in history that the U.S. has been able to do this without having to pay for it.

It's also the first time in history that the U.S. has been able to do this without having to pay for it.

Mathematical representation

In this work, as in our recent studies (Lipniacki et al., 2006 and 2007) we follow the method proposed by Haseltine and Rawlings (2002) and split the reaction channels into fast and slow, which results in a hybrid stochastic-deterministic model. We consider all reactions involving mRNA and protein molecules as fast and the reactions of receptor and gene activation and inactivation as slow. Fast reactions are approximated by the deterministic reaction-rate equations, whereas slow reactions are considered stochastic. In addition we consider the deterministic approximation of hybrid model consisting solely of the ordinary differential equations (ODEs). According to the above, the hybrid model consists of 16 ordinary differential equations accounting for:

- formation of the (I κ B α -NF- κ B) complexes,
- IKKK and IKK kinase activation and inactivation
- IKKa driven I κ B α phosphorylation,
- A20, I κ B α and phospho-I κ B α protein degradation
- transport between nucleus and cytoplasm, and
- transcription and translation.

All the substrates are quantified in number of molecules. The upper-case letters denote substrates or their complexes. Nuclear amounts are represented by subscript n, while subscript c denoting amount of substrate in the cytoplasm is omitted, to simplify the notation. Amounts of the mRNA transcripts of A20 and I κ B α are denoted by subscript t:

Notation guide:

- $\gamma^{(2)}$ IKKn - neutral form of IKK kinase,
- $\gamma^{(3)}$ IKKa - active form of IKK,
- $\gamma^{(4)}$ IKKi - inactive form of IKK,
- IKKii - inactive intermediate form of IKK,
- K_{NN} - total number of IKK=IKKn+IKKa+IKKi+IKKii molecules (assumed constant in time)
- $\gamma^{(1)}$ IKKKa - active form of IKKK,
- IKKKn - neutral form of IKKK,
- K_N - total number of IKKK=IKKKn+IKKKa molecules (assumed to be constant in time)
- $\gamma^{(10)}$ I κ B - cytoplasmic I κ B α

- $\gamma(12)$ ~~$\gamma(8)$~~ $I\kappa B_n$ - nuclear $I\kappa B\alpha$,
 $\gamma(13)$ $I\kappa B_t$ - $I\kappa B\alpha$ transcript,
 $\gamma(5)$ $I\kappa B_p$ - phosphorylated cytoplasmic $I\kappa B\alpha$
 $\gamma(14)$ $NF\kappa B|I\kappa B$ - cytoplasmic ($NF\kappa B$ - $I\kappa B\alpha$) complexes
 $\gamma(6)$ $NF\kappa B|I\kappa B_p$ - phosphorylated cytoplasmic $I\kappa B\alpha$ complexed to $NF\kappa B$
 $\gamma(15)$ $NF\kappa B|I\kappa B_n$ - nuclear ($NF\kappa B$ - $I\kappa B\alpha$) complexes
 $\gamma(16)$ TNF_{ext} - extracellular $TNF\alpha$ concentration [ng/ml],
 $G_{I\kappa B}$ - discrete random variable, state of $I\kappa B\alpha$ gene,
 G_{A20} - discrete random variable, state of $A20$ gene,
 G_R - discrete random variable, state of reporter gene,
 B - number of active receptors, M - total number of receptors (assumed to be constant in time)

$\gamma(9)$ $NF\kappa B$ nuclear
 $\gamma(7)$ $NF\kappa B$ cytoplasmic
 $\gamma(9)$ $A20$
 $\gamma(10)$ $A20$ transcription
 ~~$\gamma(6)$ TNFR1 substrate~~
 $\gamma(17)$ mRNA reporter

Table M2 Parameter set for the main model. Since all substrates are quantified in numbers of molecules the concentration does not appear in units.

symbol	value	reaction, reference
<i>The cell</i>		
$k_v = V/U$	5	ratio of cytoplasmic to nuclear volume - assumed
M_{3T3}	2×10^3	Average number of TNFR1 for 3T3 cell simulations - assumed
$M_{SK-N-AS}$	5×10^3	Average number of TNFR1 for SK-N-AS cell simulations - assumed
M_{MEFs}	10^4	Average number of TNFR1 for MEFs cell simulations - assumed
M_{HeLa}	5×10^2	Average number of TNFR1 for HeLa cell simulations - assumed
K_N	10^5	number of IKKK molecules - assumed
K_{NN}	2×10^5	number of IKK molecules - assumed
$NF\kappa B_{tot}$	10^5	average number of $NF\kappa B$ molecules (see text)
<i>TNFR1 activation and signal transduction cascade</i>		
c_{deg}	$2 \times 10^{-4} s^{-1}$	extracellular $TNF\alpha$ degradation; for simulations of cells in the microfluidic chamber these effective loss rates are used: $2 \times 10^{-4} s^{-1}$, $7 \times 10^{-4} s^{-1}$, $7.7 \times 10^{-4} s^{-1}$ and $8.3 \times 10^{-4} s^{-1}$ for 10ng/ml, 1ng/ml, 0.1ng/ml,

Negative Hill Expt

\rightarrow

Nit Hill Function \rightarrow

Not Michaelis Coefficients

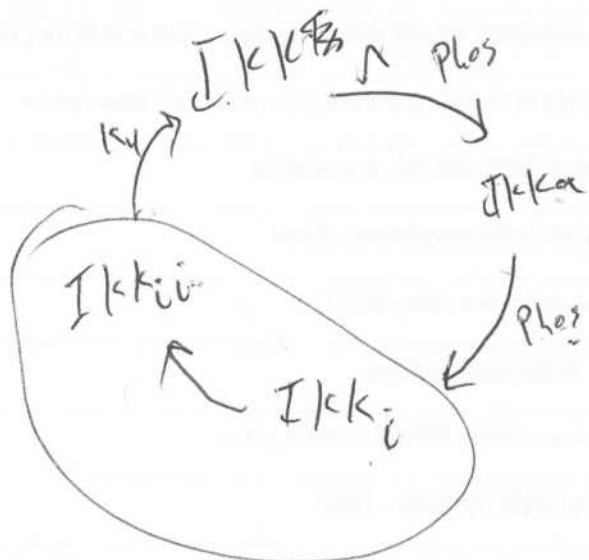
		and 0.01ng/ml respectively
k_b	$1.2 \times 10^{-5} \text{ s}^{-1} (\text{ng/ml})^{-1}$	receptor activation rate - fitted
k_f	$1.2 \times 10^{-3} \text{ s}^{-1}$	receptor inactivation rate – Grell et al., 1998
k_a	$2 \times 10^{-5} \text{ s}^{-1}$	IKKK activation rate - assumed
k_i	10^{-2} s^{-1}	IKKK inactivation rate - fitted
k_l	$6 \times 10^{-10} \text{ s}^{-1}$	IKKn activation rate - fitted
k_{A20}	10^5	Michaelis coefficient in TNFR1 activity attenuation - fitted *
k_2	10^4	Michaelis coefficient in IKKa inactivation - fitted *
k_3	$2 \times 10^{-3} \text{ s}^{-1}$	IKKn inactivation rate - fitted
k_4	10^{-3} s^{-1}	IKKi \rightarrow IKKii and IKKii \rightarrow IKKn transformation -fitted
<i>A20 and IκBα synthesis</i>		
q_1	$4 \times 10^{-7} \text{ s}^{-1}$	NF- κ B binding at A20 and I κ B α gene promoters -fitted
q_2	10^{-6} s^{-1}	I κ B α inducible NF- κ B detaching from A20 and I κ B α genes - fitted
c_1	0.1 s^{-1}	inducible A20 and I κ B α mRNA synthesis - assumption
c_3	$7.5 \times 10^{-4} \text{ s}^{-1}$	A20 and I κ B α mRNA degradation
c_4	0.5 s^{-1}	A20 and I κ B α translation - fitted
c_5	$5 \times 10^{-4} \text{ s}^{-1}$	A20 degradation rate - fitted
<i>IκBα interactions</i>		
a_1	$5 \times 10^{-7} \text{ s}^{-1}$	I κ B α association NF- κ B - assumption
a_2	10^{-7} s^{-1}	I κ B α phosphorylation - fitted
a_3	$5 \times 10^{-7} \text{ s}^{-1}$	I κ B α phosphorylation in I κ B α NF- κ B complexes - fitted
t_p	10^{-2} s^{-1}	degradation of phosphorylated I κ B α - fitted
c_{5a}	10^{-4} s^{-1}	spontaneous I κ B α degradation - assumption
c_{6a}	$2 \times 10^{-5} \text{ s}^{-1}$	spontaneous I κ B α degradation in I κ B α NF- κ B complexes - assumption

$$\frac{A_{20}}{k_{A20} + A_{20}} = \frac{k_{A20}}{k_{A20} + A_{20}} \neq \frac{A_{20}}{k_{A20} + A_{20}}$$

$$k_A B(t) \cdot I \ll k_{k_n}$$

$$1 - \frac{A_{20}}{k_{A20} + A_{20}}$$

$$\frac{A_{20}}{k_{A20} + A_{20}} \cdot k_A B(t) \cdot I \ll k_{k_n}$$



Transport		
i_1	10^{-2} s^{-1}	NF-κB nuclear import
e_{2a}	$5 \times 10^{-2} \text{ s}^{-1}$	IκBα NF-κB nuclear export
i_{1a}	$2 \times 10^{-3} \text{ s}^{-1}$	IκBα nuclear import
e_{1a}	$5 \times 10^{-3} \text{ s}^{-1}$	IκBα nuclear export
Reporter gene parameters		
q_{1r}	10^{-7} s^{-1}	NF-κB binding at reporter gene promoter
q_{2r}	10^{-7} s^{-1}	IκBα inducible NF-κB detaching from reporter gene
q_{2rr}	10^{-3} s^{-1}	spontaneous NF-κB detaching from reporter gene
c_{1r}	$5 \times 10^{-2} \text{ s}^{-1}$	inducible reporter mRNA synthesis
c_{1rr}	10^{-3} s^{-1}	reporter mRNA constitutive synthesis
c_{3r}	various	reporter mRNA degradation rate

ODEs

IKKK in active state (IKKKA): the first term describes IKKK kinase activation, i.e. transformation from IKKKn (amount of which is $\text{IKKK}_n = K_N - \text{IKKKA}_n$) due to action of active receptors $B(t)$, whose activity is attenuated by $A20$. The second term describes spontaneous inactivation of the kinase:

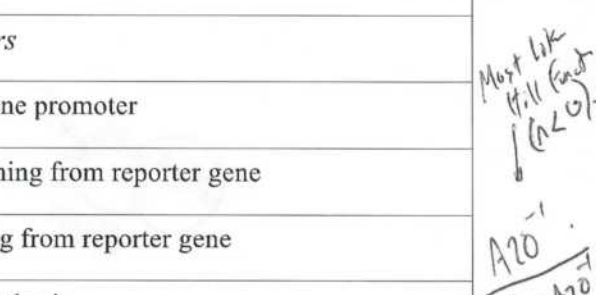
$$\frac{d}{dt} \text{IKKKA}(t) = k_a \times B(t) \times (K_N - \text{IKKKA}(t)) \times k_{a20} / (k_{a20} + A20) - k_i \times \text{IKKKA}(t)$$

IKK in neutral state (IKKn): the first term describes recovery from the state IKKii (amount of which is $\text{IKK}_{ii} = K_{NN} - \text{IKK}_n - \text{IKK}_a - \text{IKK}_i$) second depletion due to activation by IKKKA (since IKK must be phosphorylated at two serine residues 177 and 181 the second order reaction is assumed):

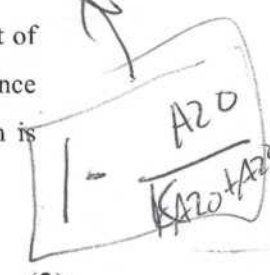
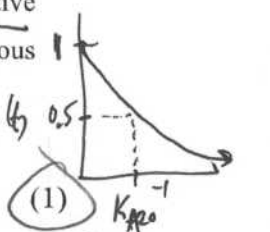
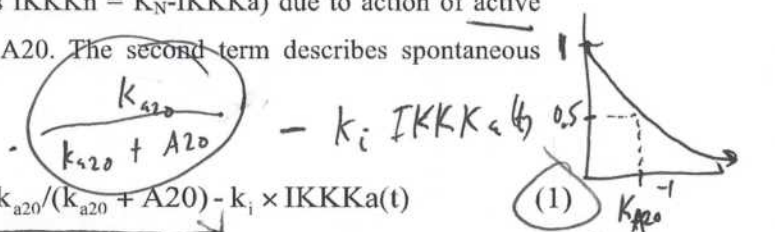
$$\frac{d}{dt} \text{IKKn}(t) = k_4 \times (K_{NN} - \text{IKK}_n - \text{IKK}_a - \text{IKK}_i) - k_1 \times \text{IKKKA}(t) \times \text{IKKn}(t)$$

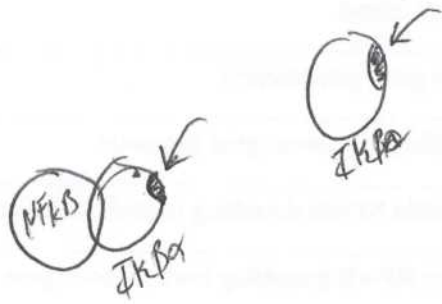
$$k_4 \cdot \text{IKK}_{ii} - k_1 \cdot \text{IKKKA}_n^2 \cdot \text{IKKn}$$

Net from both ends



clock Term $\rightarrow \left(\frac{A20^{-1}}{\frac{1}{k_{a20}} + A20^{-1}} \right)$





IKK in the active state IKKa: The first term represents transition from IKKi to IKKa mediated by IKK α , whereas the second term represents depletion of IKKa due to its transformation into inactive form IKKi mediated by A20 (since IKK must be phosphorylated at two serine residues 177 and 181 the second order reaction is assumed):

$$\frac{d}{dt} \text{IKKa}(t) = k_1 \times \text{IKK}\alpha^2(t) \times \text{IKKn}(t) - k_3 \times \text{IKKa}(t) \times (k_2 + A20(t))/k_2$$

1st Hill function

Loyd's law term

$$\left(1 + \frac{A20}{k_2}\right)$$

or

$$\left(\frac{k_2}{k_2 + A20}\right)^{-1}$$

IKK in the inactive state IKKi: The first term corresponds to the formation of inactive IKKi from IKKa by A20 mediated inactivation, whereas the second term describes transformation into IKKi β :

$$\frac{d}{dt} \text{IKKi}(t) = k_3 \times \text{IKKa}(t) \times (k_2 + A20(t))/k_2 - k_4 \times \text{IKKi}(t)$$

Use conservation law for IKKi β

Phospho-I κ B α (IkB p): The first term describes IkB α phosphorylation due to catalytic action of IKKa, the second term catalytic degradation of phosphorylated IkB α :

$$\frac{d}{dt} \text{IkB}_p(t) = a_2 \times \text{IKKa}(t) \times \text{IkB}(t) - t_p \times \text{IkB}_p(t) \quad (5)$$

Phospho-I κ B α complexed to NF- κ B (NFkB|IkB p): The first term describes IkB α phosphorylation (in complexes with NF- κ B) due to the catalytic action of IKKa, the second term catalytic degradation of phosphorylated IkB α (NF- κ B is recovered):

$$\frac{d}{dt} (\text{NFkB}| \text{IkB}_p)(t) = a_3 \times \text{IKKa}(t) \times (\text{NFkB}| \text{IkB})(t) - t_p \times (\text{NFkB}| \text{IkB}_p)(t) \quad (6)$$

Free cytoplasmic NF- κ B: The first two terms represents liberation of free NF- κ B due to degradation of IkB α in (NFkB|IkB) complexes and its depletion due to formation of these complexes. The third term accounts for liberation of NF- κ B due to degradation of phospho-IkB α .

The last term describes transport of free cytoplasmic NF- κ B to the nucleus:

$$\begin{aligned} \frac{d}{dt} \text{NFkB}(t) = & c_{6a} \times (\text{NFkB}| \text{IkB})(t) - a_1 \times \text{NFkB}(t) \times \text{IkB}(t) + t_p \times (\text{NFkB}| \text{IkB}_p)(t) \\ & - i_1 \times \text{NFkB}(t) \end{aligned} \quad (7)$$

IkB to nucleus

NF- κ B bin from complex degradation

Complex Formation (Lns)

Free nuclear NF-κB: The first term describes transport into the nucleus. The second term represents depletion of free nuclear NF-κB due to the association with nuclear IκBα and is adjusted, by multiplying the synthesis coefficient a_1 by $k_v = V/U$ to the smaller nuclear volume:

$$\frac{d}{dt} NFkB_n(t) = \underbrace{i_1 \times NFkB(t)}_{\text{Gene}} - \underbrace{a_1 \times k_v \times IkB_n(t) \times NFkB_n(t)}_{\text{Complex Formation}} \xrightarrow{5} \underbrace{\text{NFkB}_n}_{\substack{\text{Cytoplasm} \\ \text{Nucleus}}} \quad (8)$$

5 times more
likely in smaller
space

A20 protein: Described by its synthesis and constitutive degradation:

$$\frac{d}{dt} A20(t) = \underbrace{c_4 \times A20(t)}_{\substack{\text{RNA} \\ \text{Production}}} - \underbrace{c_5 \times A20(t)}_{\text{Decay}} \quad (9)$$

RNA
Production
Decay

A20 transcript: The first term stands for NF-κB inducible synthesis, while the second term describes degradation of the A20 transcript:

$$\frac{d}{dt} A20_t(t) = \underbrace{c_1 \times G_{A20}(t)}_{\substack{\text{Transcription} \\ \text{Inducible}}} - \underbrace{c_3 \times A20_t(t)}_{\text{Decay}} \quad (10)$$

NA Gene State
 $G_{A20} \in [0, 1/2]$
Transcription
Decay
Inducible
const & small.

Note that Eq. (10) (as well as Eq. 13) naturally produces saturation in transcription speed. When the nuclear amount of regulatory factor NF-κB is very large, then the binding probability is much larger than the dissociation probability, and the gene state would be $G_{A20} = 2$ for most of the time. In such case the transcription would proceed at a maximum rate, $2 c_1$.

Free cytoplasmic IκBα protein: The first term accounts for IKKα induced phosphorylation, the second for NF-κB binding. The second line describes IκBα synthesis and the constitutive degradation of IκBα. The last two terms represent transport into and out of the nucleus:

$$\begin{aligned} \frac{d}{dt} IkB(t) = & \underbrace{-a_2 \times IKKa(t) \times IkB(t)}_{\substack{\text{Loss from Phosphorylation}}} - \underbrace{a_1 \times IkB(t) \times NFkB(t)}_{\substack{\text{Complex Formation}}} \\ & + c_4 \times IkB_t(t) - \underbrace{c_{5a} \times IkB(t)}_{\text{Decay}} - \underbrace{i_{1a} \times IkB(t)}_{\text{To Nuclear Loss}} + \underbrace{e_{1a} \times IkB_n(t)}_{\text{From Nuclear Gain}} \end{aligned} \quad (11)$$

Loss from Phosphorylation
Complex Formation
Production
Decay
To Nuclear Loss
From Nuclear Gain

Free nuclear IκBα protein: The first term corresponds to IκBα association with nuclear NF-κB (adjusted, by multiplying the synthesis coefficient a_1 by $k_v = V/U$ for the smaller nuclear volume resulting in larger concentration), and the last two terms represent the transport into and out of the nucleus:

$$\frac{d}{dt} I\kappa B_n(t) = \underbrace{-a_1 \times k_v \times I\kappa B_n(t) \times NF\kappa B_n(t)}_{\text{Complex Formation}} + \underbrace{i_{1a} \times I\kappa B(t)}_{\text{To cytosol}} - \underbrace{e_{1a} \times I\kappa B_n(t)}_{\text{From Nucleus Loss}} \quad (12)$$

IκBα transcript: The first term stands for NF-κB inducible synthesis, whereas the second term describes transcript degradation:

$$\frac{d}{dt} I\kappa B_t(t) = \underbrace{c_1 \times G_{I\kappa B}(t)}_{\text{RNA Production}} - \underbrace{c_3 \times I\kappa B_t(t)}_{\text{Decay}} \quad (13)$$

Cytoplasmic (NFκB|IκB) complexes: The first two term describes formation of the complexes due to IκBα and NF-κB association and their degradation. The third term represents phosphorylation of (NFκB|IκB) complexes due to the catalytic activity of IKKα. The last term represents transport of the complex from the nucleus:

$$\begin{aligned} \frac{d}{dt} (NF\kappa B | I\kappa B)(t) &= \underbrace{a_1 \times I\kappa B(t) \times NF\kappa B(t)}_{\text{Complex Formation}} - \underbrace{c_{6a} \times (NF\kappa B | I\kappa B)(t)}_{\text{IKBα Decay in Cytosol}} \\ &- \underbrace{a_3 \times IKK\alpha(t) \times (NF\kappa B | I\kappa B)(t)}_{\text{Degradation}} + \underbrace{e_{2a} \times (NF\kappa B | I\kappa B_n)(t)}_{\text{From Nucleus}} \end{aligned} \quad (14)$$

Nuclear (NFκB|IκB_n) complexes: Described by their formation due to IκB_n and NF-κB_n association adjusted, by multiplying the synthesis coefficient a_1 by $k_v = V/U$, to the smaller nuclear volume resulting in larger concentration) and their transport out of the nucleus:

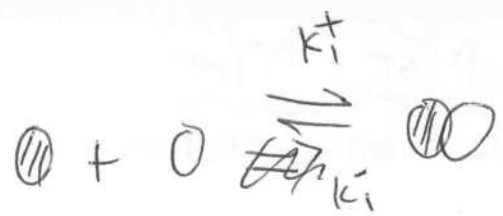
$$\frac{d}{dt} (NF\kappa B | I\kappa B_n)(t) = \underbrace{a_1 \times k_v \times I\kappa B_n(t) \times NF\kappa B_n(t)}_{\text{Complex Formation}} - \underbrace{e_{2a} \times (NF\kappa B | I\kappa B_n)(t)}_{\text{From Nucleus Loss}} \quad (15)$$

Extracellular TNFα concentration: The concentration decreases due to natural degradation and binding to TNFR1 receptors:

$$\frac{d}{dt} TNF_{ext}(t) = -k_{deg} \times TNF_{ext}(t) \rightarrow k_b \cdot TNF_{ext}(t) \cdot TNFR \quad (16)$$

Propensities of receptors and genes activation and inactivation

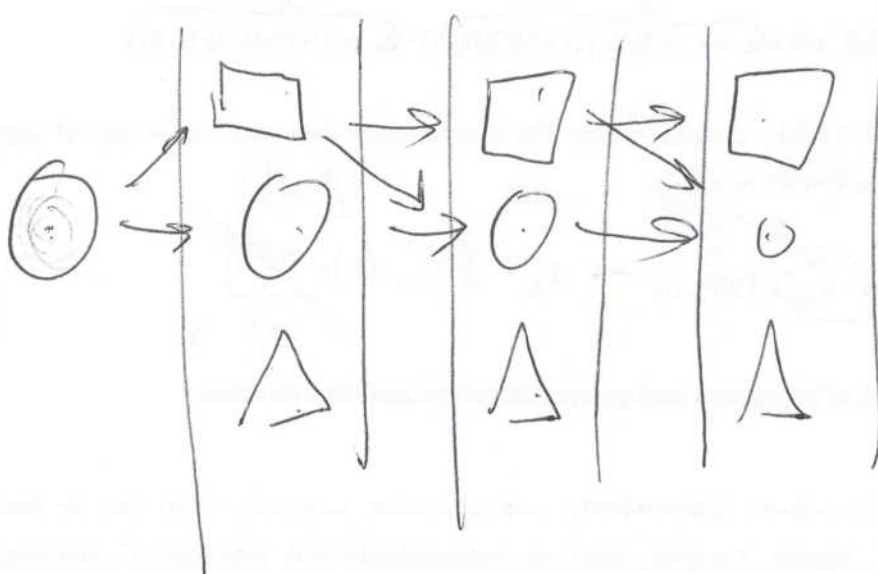
The receptors activate independently with activation propensity $r_r^b(t)$ due to binding of extracellular ligands. Receptors inactivate independently with propensity r_r^d constant, due to dissociation of ligands or internalization of receptors:



$$\frac{d[\text{O}]}{dt} = -k_i^+ [\text{O}] [\text{O}] + k_i^- [\text{OO}]$$

$\underbrace{-k_i^+ [\text{O}] [\text{O}]}$
 Rate constant
 Reactor for O

$$\text{is } \underbrace{-k_i^+ [\text{O}]}_{\text{Propensity}}$$



$$r_r^b(t) = k_b \times \text{TNF}_{\text{ext}}(t); \quad r_r^d = k_d$$

(17)

We assume that both A20 and I κ B α genes have two homologous copies independently activated due to NF- κ B binding, and inactivated due I κ B α mediated removal of NF- κ B molecules, and that binding and dissociation propensities $r^b(t)$ and $r^d(t)$ respectively, are equal for each copy:

$$r^b(t) = q_1 \times \text{NFkB}_n(t); \quad r^d(t) = q_2 \times \text{IkB}_n(t) \quad (18)$$

The state of gene copy G^i ($i = 1, 2$) is $G^i = 1$ whenever NF- κ B is bound to the promoter regulatory site, and $G^i = 0$ when the site is unoccupied. As a result the gene state $G = G^1 + G^2$ can be equal to 0, 1 or 2.

0, 1, 2

Deterministic Approximation

In the deterministic approximation of the hybrid model the evolution of number of active receptors and of gene states are governed by the following deterministic equations:

Number of active TNFR1 receptors B: The first term describes receptor activation due to binding of TNF α trimers, while the second one describes their inactivation due to dissociation or internalization of receptors. For the sake of simplicity we assume that internalized receptors are replenished by novo synthesis:

$$\frac{d}{dt} B(t) = k_b \times \text{TNF}_{\text{ext}}(t) \times (M - B) - k_d \times B \quad (19)$$

Bin
Number of Receptors per cell
Dissociation

The state of A20 and I κ B α genes G_{A20} and $G_{I\kappa B}$: The first term describes A20 or I κ B α genes activation due to NF- κ B binding, while the second one their inactivation due to removal of NF- κ B molecules by I κ B α :

$$\frac{d}{dt} G(t) = q_1 \times \text{NFkB}_n(t) \times (2 - G) - q_2 \times \text{IkB}_n(t) \times G \quad (20)$$

Up
Down
Activation
Inactivation

Reporter gene kinetics

The state of reporter gene: We assume that all reporter genes (i.e. NF- κ B responsive genes) have two homologous copies independently activated due to NF- κ B binding, and inactivated due to spontaneous dissociation or I κ B α mediated removal of NF- κ B molecules, and that binding and dissociation propensities $r_R^b(t)$ and $r_R^d(t)$, respectively, are equal for each copy:

$$r_R^b(t) = q_{1R} \times \text{NFkB}_n(t); \quad r_R^d(t) = q_{2RR} + q_{2R} \times \text{IkB}_n(t) \quad (21)$$

As a result reporter gene state $G_R = G_R^1 + G_R^2$ can be equal to 0, 1 or 2 with respect to the number of activated copies.

Reporter gene mRNA: The first two terms describes NF- κ B independent and dependent synthesis, while the last one is mRNA degradation:

$$\frac{d}{dt} R_t(t) = c_{IRR} + c_{IR} \times G_R - c_{3R} \times R_t(t) \quad (22)$$

Inductive
Inactivating
Depend

As a result, the mRNA kinetics of any reporter gene is governed by 6 independent parameters (specific for a given gene); q_{1R} ; q_{2RR} ; q_{2R} ; c_{IRR} ; c_{IR} ; c_{3R} . The first three describe gene activation and inactivation kinetics, while the next three NF- κ B independent and dependent synthesis and mRNA degradation. Most (but not all) of the mRNA time profiles observed in this study can be explained *only* by varying the mRNA degradation parameter c_{3R} .

Numerical implementation for the stochastic model

In model computations, the amounts of all the substrates are expressed as the numbers of molecules. Since we use the ODEs to describe most of the model kinetics, amounts of molecules are not integer numbers, but since these numbers are in most cases much greater than 1, such description is reasonable. The numerical scheme implemented follows that of Lipniacki et al. (2007):

- (1) At simulation time t ; for given states $G_{A20} = G_{A20}^1 + G_{A20}^2$, $G_{IkB} = G_{IkB}^1 + G_{IkB}^2$, and $G_R = G_R^1 + G_R^2$ of the A20, I κ B α , and reporter genes, and number of active (bound)

$$\begin{bmatrix} 1 \\ 2 \\ 3 \\ \vdots \\ 1 \end{bmatrix}$$

Total Reactions
"Likelihood"

receptors B (with M equal to the total number of receptors) we calculate the total propensity function $r(t)$ of occurrence of any of the activation and inactivation reactions

$$r(t) = r_r^b \times (M - B) + r_{A20}^b(t) \times (2 - G_{A20}) + r_{IkB}^b(t) \times (2 - G_{IkB}) + r_R^b(t) \times (2 - G_R) \\ + r_r^d \times B + r_{A20}^d(t) \times G_{A20} + r_{IkB}^d(t) \times G_{IkB} + r_R^d(t) \times G_R$$

(2) We select two random numbers p_1 and p_2 from the uniform distribution on $[0, 1]$.

(3) Using the fourth order MATLAB solver we evaluate the system of ODEs accounting for fast reactions, until time $t+\tau$ that:

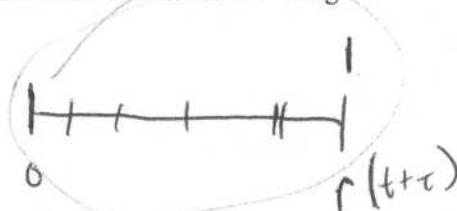
$$\log(p_1) + \int_t^{t+\tau} r(s) ds = 0$$

(4) There are 10 possible reactions:

- a) Receptors may be activated or inactivated. Typically, there are many inactive receptors which may be activated and active receptors which may be inactivated, but since the receptors are assumed to be identical it is not important which one of them changes its state.
- b) NF- κ B may bind to or dissociate from any of two alleles of A20, IkBa, or reporter genes.

In this step we determine which one of 10 potentially possible reactions occurs at time $t+\tau$ using the inequality

$$\sum_{i=1}^{k-1} r_i(t+\tau) < p_2 \times r(t+\tau) < \sum_{i=1}^k r_i(t+\tau) \quad (25)$$



where $r_i(t+\tau)$, $i=1,\dots,10$ are individual reaction propensities and k is the index of the reaction to occur.

(5) Finally time $t+\tau$ is replaced by t and we go back to item (1).

$$t = t + \tau \xrightarrow{\text{loop back}}$$

In all simulations, we simulate a resting cell for time t randomly chosen from the interval of 10 to 20 hours in order to get equilibrated and randomized initial conditions.

Model fitting and parameters

The validation of the proposed model is based on our comprehensive single cell, microfluidic chamber experiments, and additionally on major experiments of other researchers that account for different aspects of NF- κ B regulatory pathway kinetics:

This study

- Single cell nuclear NF- κ B temporal profiles for tonic TNF α stimulation (TNF α doses from 0.01 to 100 ng/ml)
- Fraction of responding cells versus TNF α dose

Previous studies

- Detailed IKK activity profile (HeLa), Delhase et al. (1999)
- Wild type and A20 $^{-/-}$ cells, IKK activity, A20 mRNA, Nuclear NF- κ B, (MEFs) Lee et al. (2000), see Fig. M6 for IKK activity and nuclear NF- κ B profiles
- System responses to short TNF α pulses in MEFs, Hoffmann et al. (2002), Werner et al. (2008), see Fig. M3 for 1, 2, 5, 15 and 45 min.
- Short pulse-pulse experiments – recovery of IKK activity (HeLa), Lipniacki et al. (2007)
- Single cell pulse-pulse-pulse and tonic stimulation – Nuclear NF- κ B measurements in SK-N-AS and HeLa (tonic stimulation only), Nelson et al. (2004), Ashall et al. (2009), see Figs. M4 and M5

When comparing the model predictions with other experiments one should keep in mind that some kinetic features of responses and NF- κ B pathway are cell specific. Cell lines exhibit a substantial difference in sensitivity to stimulation; for example MEFs appear to be about 10 times more sensitive than 3T3 cells. 3T3 cells are more sensitive than HeLa cells that exhibit only one NF- κ B peak under tonic stimulation. These differences may result from different numbers of TNFR1 receptors, IKKK or IKK levels – and the current knowledge do not allow to determine at which level of signal transduction the differences in cell sensitivity arise. Thus, for the sake of simplicity and to account for different cell lines sensitivity we assumed that cells from these lines

and the principles of the new model. This paper is the second in a series of four papers that will introduce the new model, discuss its potential benefits, and demonstrate its use.

Introduction and Model Description

The new model is designed to be used in both business and government settings. It is intended to help organizations better understand their needs and goals, and to provide them with the tools they need to achieve those goals.

Model Overview

The new model consists of three main components: Business Model, Government Model, and Social Model.

Business Model

The Business Model component of the new model is designed to help organizations better understand their needs and goals, and to provide them with the tools they need to achieve those goals.

Government Model

The Government Model component of the new model is designed to help organizations better understand their needs and goals, and to provide them with the tools they need to achieve those goals.

Social Model

The Social Model component of the new model is designed to help organizations better understand their needs and goals, and to provide them with the tools they need to achieve those goals.

Conclusion

This paper has introduced the new model, which is designed to help organizations better understand their needs and goals, and to provide them with the tools they need to achieve those goals. The new model is based on the principles of the old model, but it is more flexible and easier to use. It also includes new features, such as the ability to define goals and objectives, and to track progress towards those goals. The new model is intended to be used by both business and government organizations, and it is hoped that it will be adopted by many organizations around the world. The new model is a significant improvement over the old model, and it is expected to have a positive impact on the way organizations operate.

have different numbers of TNFR1 receptors; HeLa: 500; 3T3: 2000; SK-N-AS 5000; MEFs: 10000 receptors each.

The population studies of NF- κ B by the groups of Baltimore, Levchenko and Hoffmann, or single cell experiments performed by White and colleagues were all performed in cell culture wells. The most important difference between such well and microfluidic chambers is the much larger media volume per cell in the wells, which determines the available number of molecules per cell at a given dose. As shown in Fig. M.2 the number of TNF α -TNFR1 complexes, depends not only on the initial concentration but also on the media volume per cell.

We do not fit the parameters to any given single experiment using automatic fitting procedures like the one proposed by Fujarewicz et al. (2007), but we intuitively choose the set of parameters which produces qualitative agreement with a major subset of existing data. Because of a large number of undetermined parameters, this is a tedious task, but in our opinion it is better to produce a model in qualitative agreement with the current and previous experiments, than a model perfectly fitted to a single experiment with limited set of data.

We based our choice of parameters on both single cell and population experiments. To compare our model with population based experiments, we average a large number of single-cell stochastic simulations. This procedure is much more time consuming than comparing the deterministic model with the population data, but as already shown in the case of low dose TNF α stimulation, the population data do not correspond to any biological process, and thus constructing the model fitted to such data is not justified.

We applied the following method of choosing the parameter values:

- 1) Start from a reasonable set of parameters, which produces a correct steady state in the absence of TNF α signal.
- 2) Proceed with the signal initiated by downstream the autoregulatory loops.
- 3) Iterate item 2 until the fit to all the data is satisfactory.

As stated in item 2, we first fit the coefficients regulating IKK activation using existing data on IKK activity, then the coefficients regulating degradation of the cytoplasmic (I κ B α |NF- κ B) and I κ B α degradation, and so forth. It is necessary to iterate the signal tracing several times, until the

fit is satisfactory. We find that the set of parameters is that produce a satisfactory fit is not unique. This ambiguity is mainly caused by the lack of measurements of absolute values of protein or mRNA amounts. The action exerted by some components of the pathway onto the rest of the pathway is determined by their amounts multiplied by undetermined coupling coefficients. Hence, once a good set of parameters is found, another one can also be produced using, for example, a smaller coupling coefficient and by proportionately enlarging the absolute level of the component. Since not all parameters may be determined based on existing data we have assumed values of part of parameters mostly based on our intuition and fitted the remaining ones. By such approach we show how much information can be inferred from available experimental data. Ambiguity in parameter determination leads to significant differences between parameters of our model and the corresponding parameters chosen by others groups of researcher. Values of all model parameters are used in our model is listed in Table M2.

FIGURES

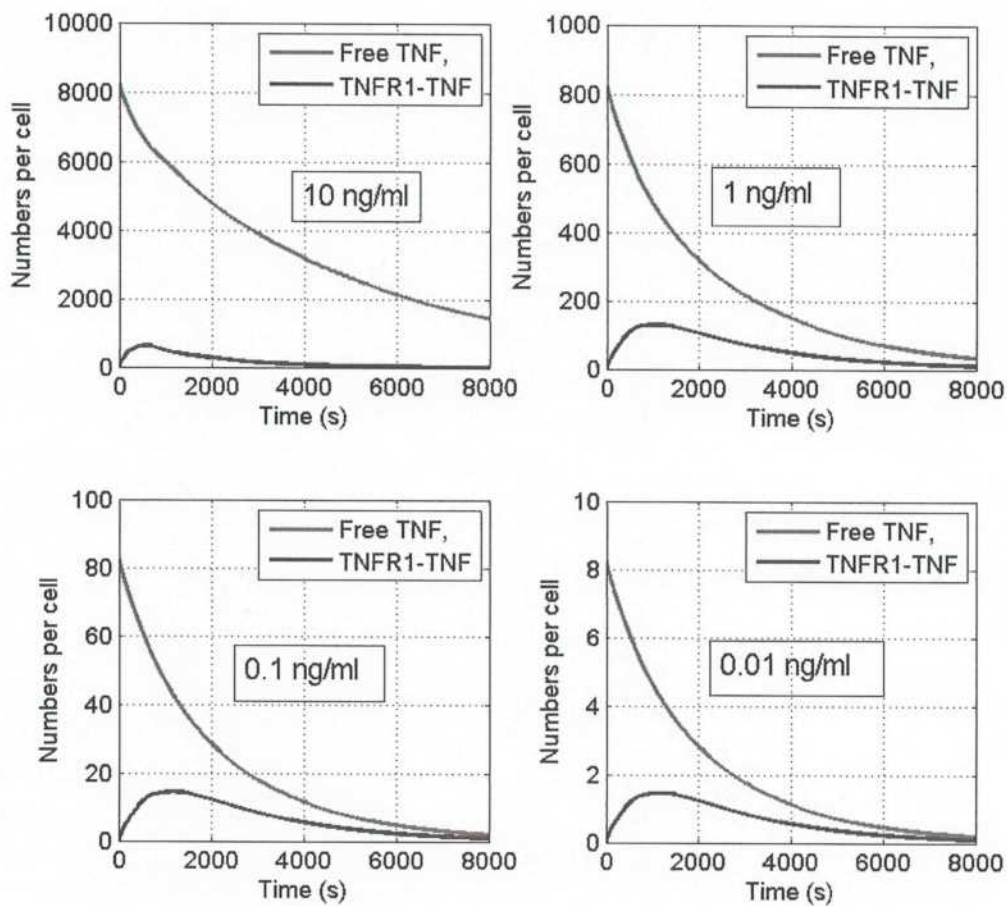


Fig. M1 Number of free and bound TNF α molecules per cell for four initial TNF α concentrations: 10, 1, 0.1, and 0.01 ng/ml.

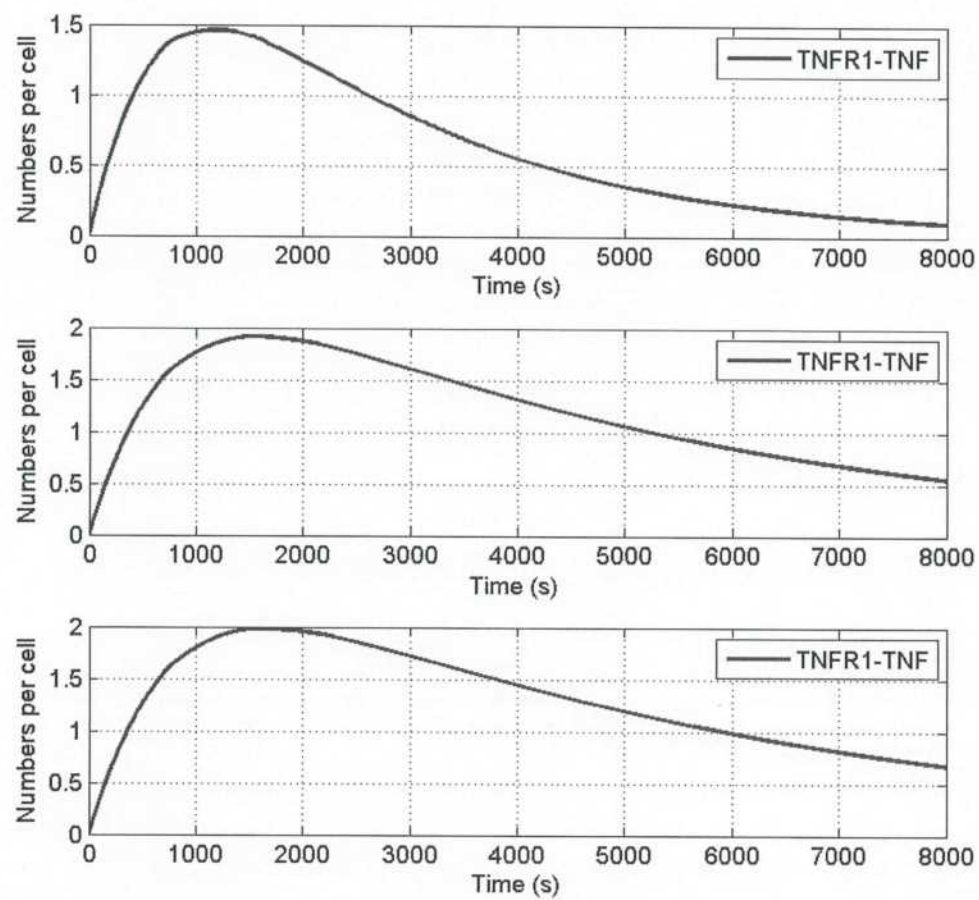
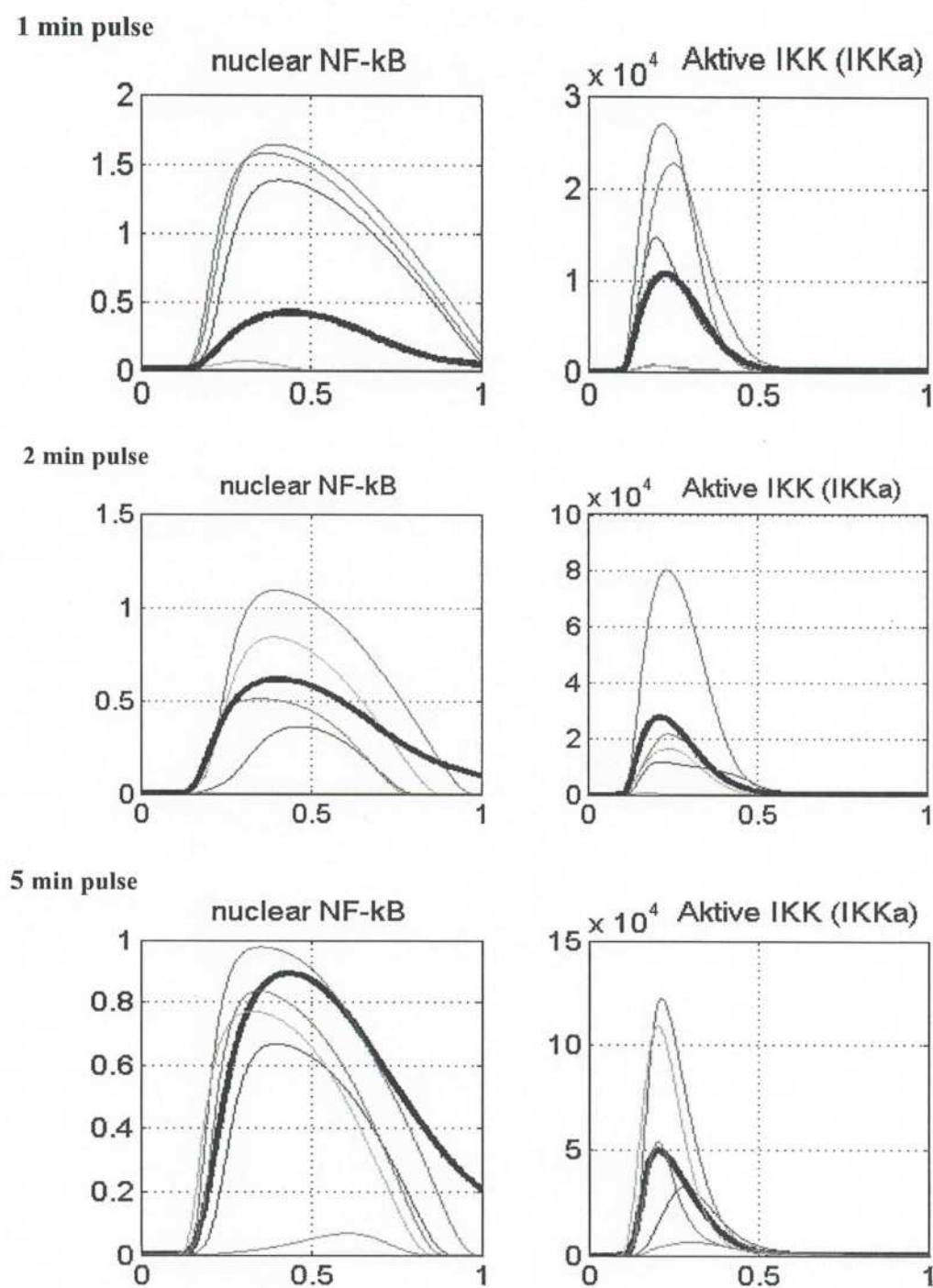
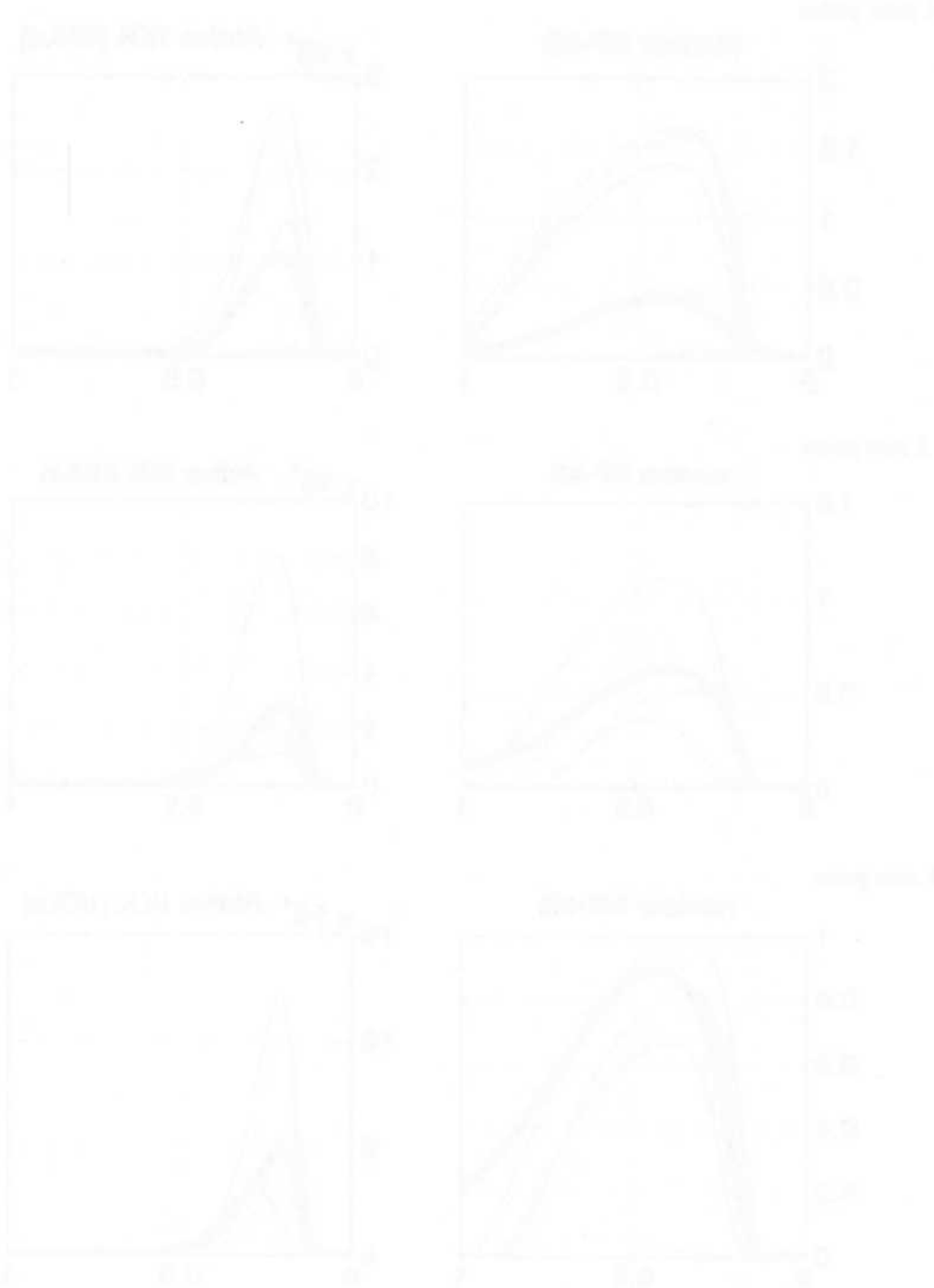
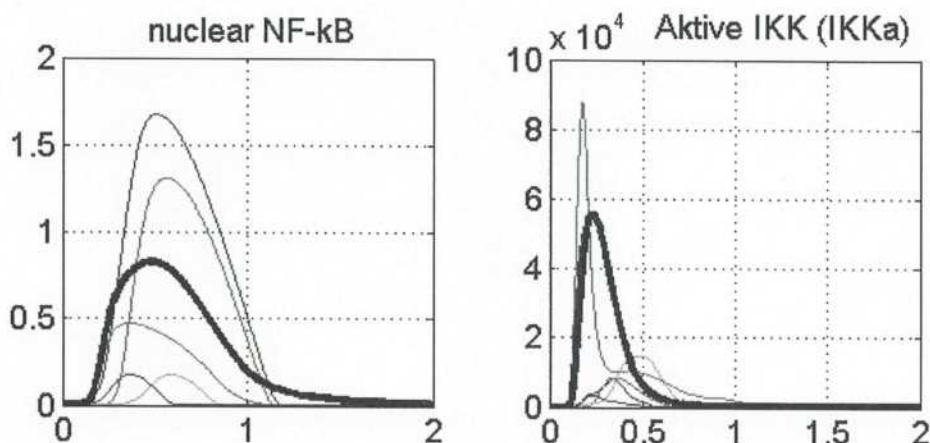


Fig. M2 Number bound TNF α molecules per cell for initial TNF α concentration 0.01 ng/ml in the 35 nanoliter microfluidic chamber, and chambers having 10 times and 100 times larger volume but containing the same number of cells.





15 min pulse



45 min pulse

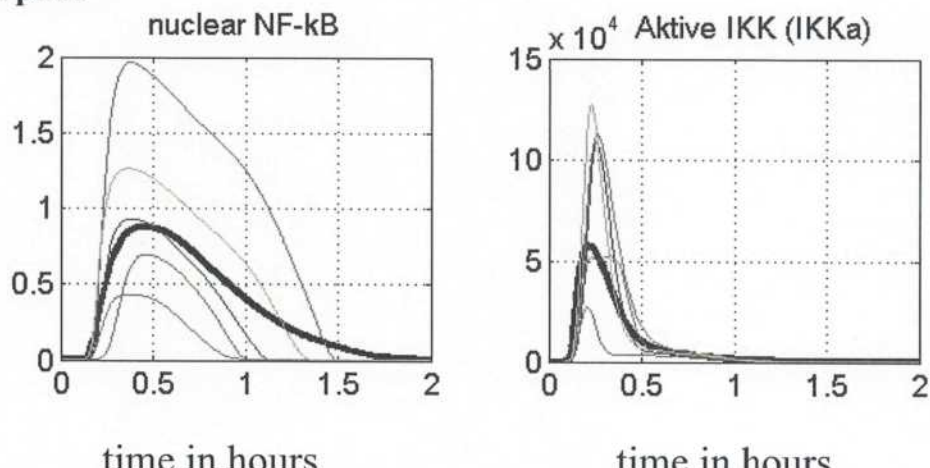


Fig. M3 Numerical simulations of short-pulsed stimulations of MEFs (10000 TNFR1). Cells are stimulated by 1, 2, 5, 15 and 45 minute long 1ng/ml TNF α pulses, Bold black line: average over 100 cells, thin lines: single cell stochastic trajectories. Nuclear NF- κ B is given in 10^5 molecules. The 1 min long 1ng/pulse is sufficient to activate most of the cells, as observed by Werner et al. (2008). The responses to 15 and 45 min pulses are in agreement with Hoffman et al. 2002 experiment.

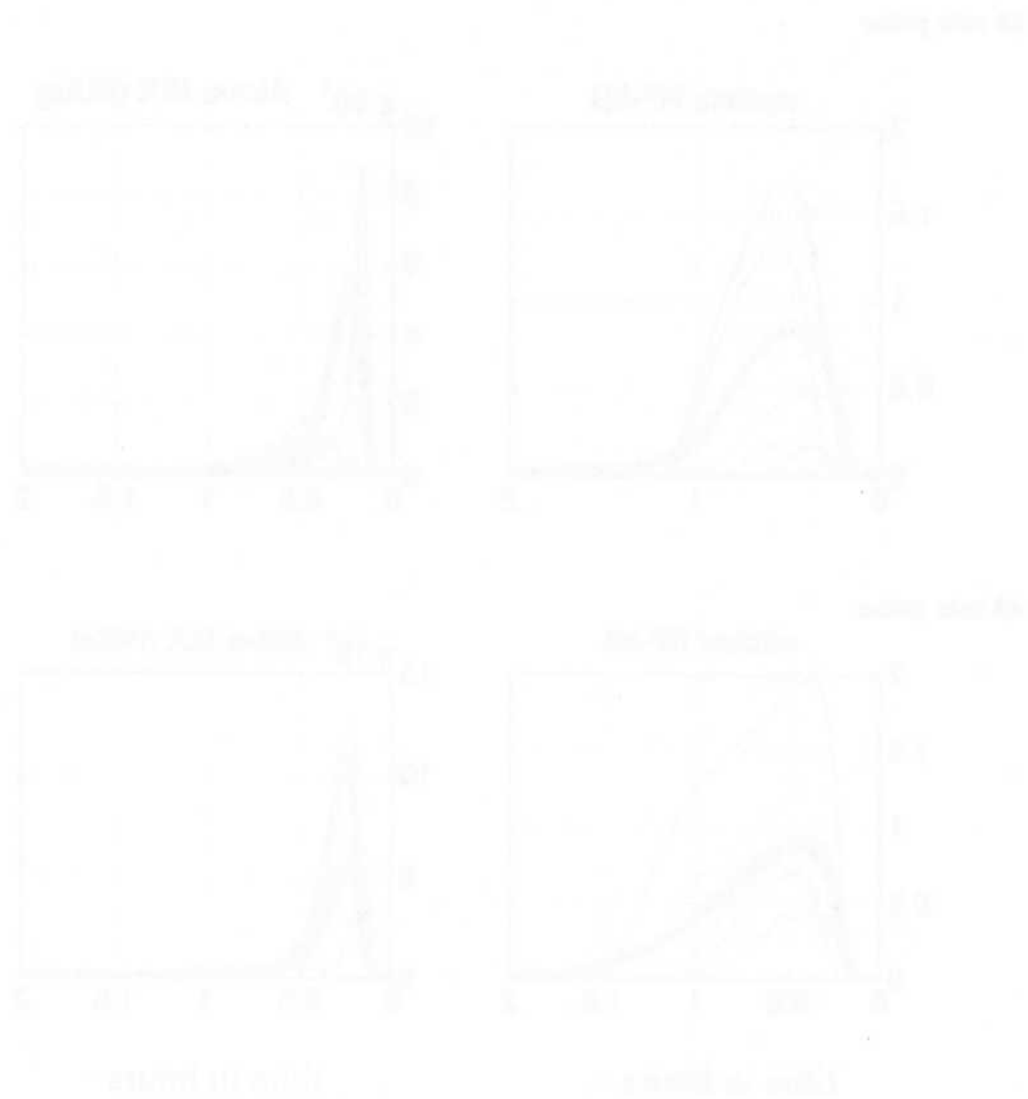


Fig. 2 Relationship between body condition (BC) and growth rate (GR) for four groups. The top row shows BC on the y-axis, and the bottom row shows GR on the y-axis. The left column shows BC on the y-axis, and the right column shows BC on the x-axis. The x-axis for all graphs is 'growth rate' (GR), ranging from 0 to 10. The curves show that BC increases with GR up to a peak value, after which it decreases. The peak value of BC is higher for older males than for young males, and for older females than for young females. The peak value of BC is also higher for males than for females

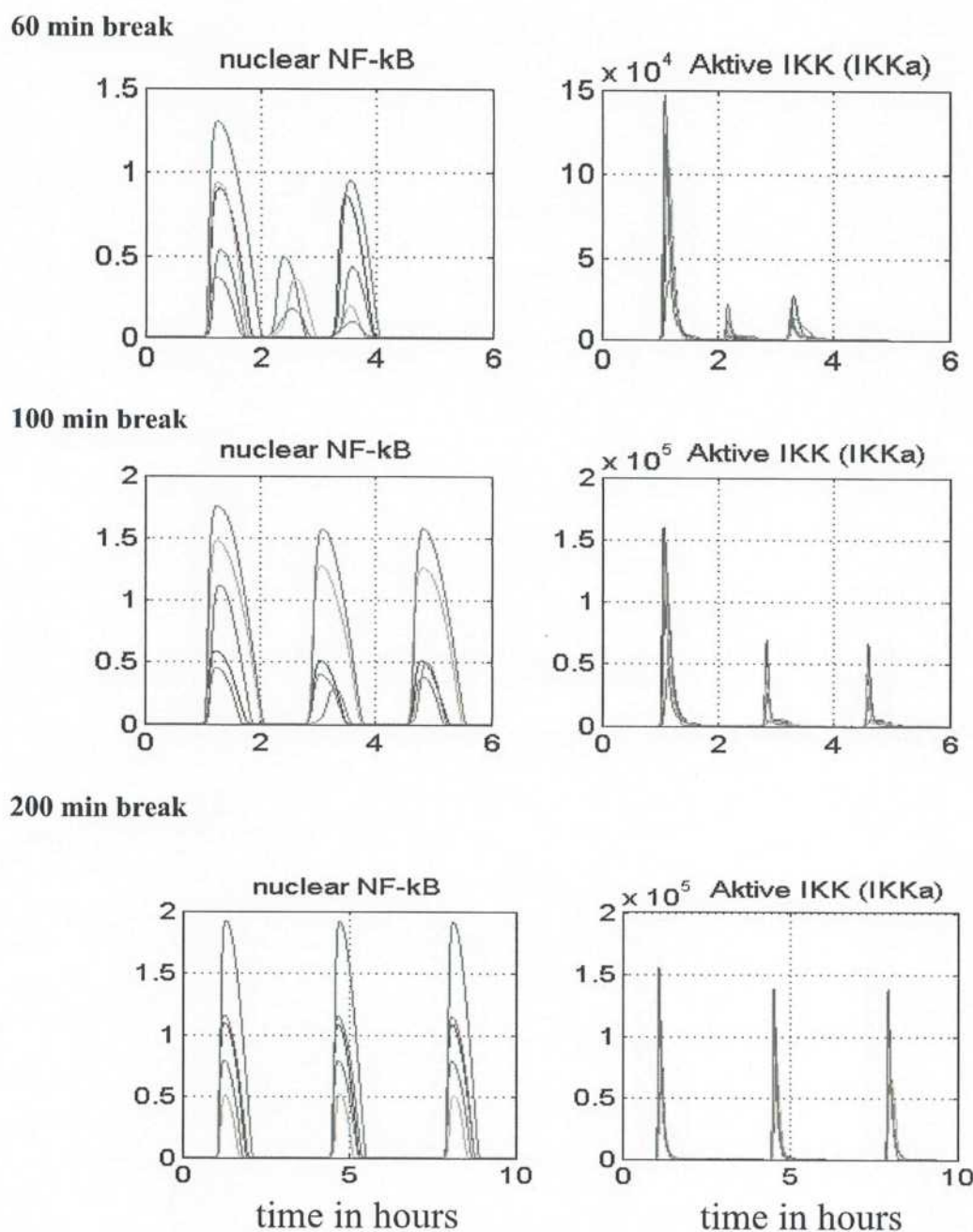
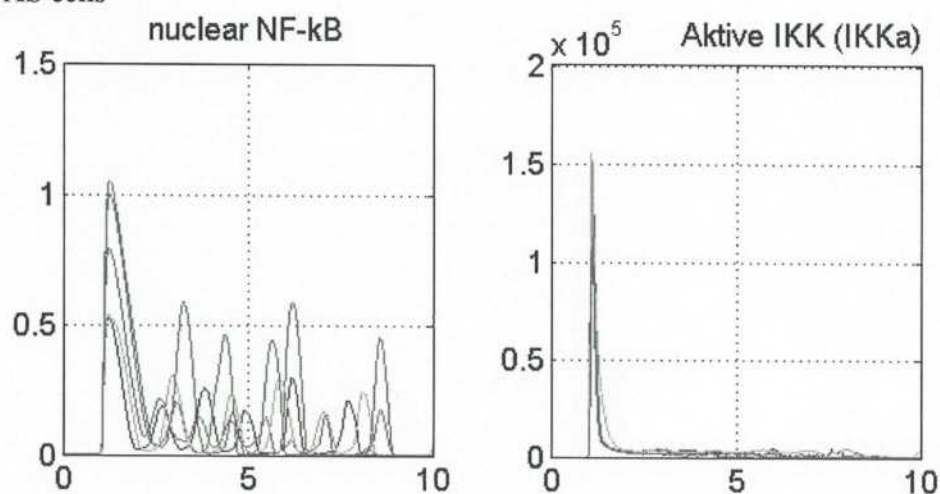


Fig. M4 Simulations of three consecutive short-pulses of TNF α stimulation (Pulse-Pulse-Pulse) on SK-N-AS cells (5000 TNFR1). Cells were stimulated by three, five minutes long, 10ng/ml pulses separated by respectively 60, 100 min and 200 min breaks. Nuclear NF-κB is given in 10^5 molecules. The results are in good agreement with Ashall et al. (2009) and Lipniacki et al., (2007, IKK activity).

SK-N-AS cells



HeLa cells

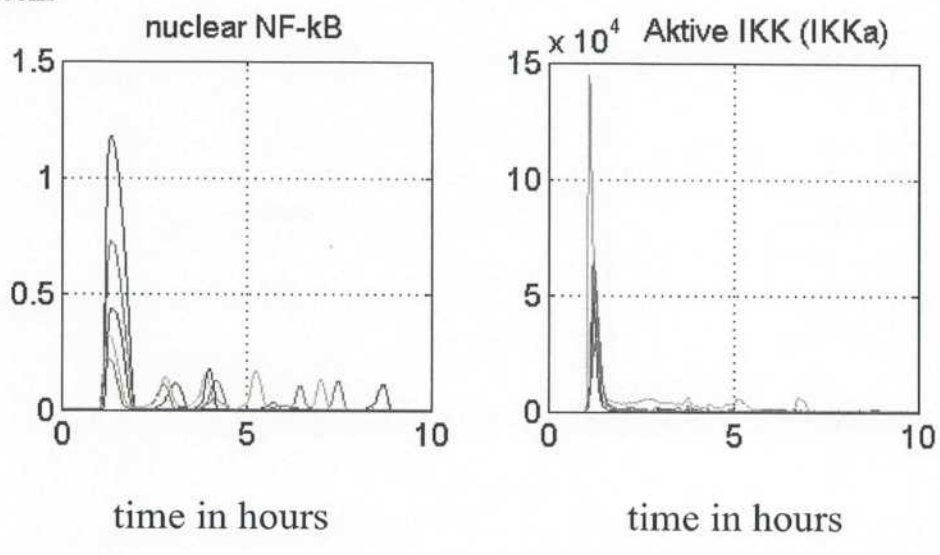


Fig. M5 Simulated tonic stimulation of SK-N-AS and HeLa cells by 10ng/ml TNF α , where each cell type is assumed to have 5000 and 500 TNFR1 receptors, respectively (see Nelson et al., 2004). Nuclear NF- κ B is given in 10^5 molecules. The high sensitivity to TNF α in SK-N-AS cells results in multiple oscillations, while the low sensitivity in HeLa cancer cell line results in reduced NF- κ B activity.

Wild type cells

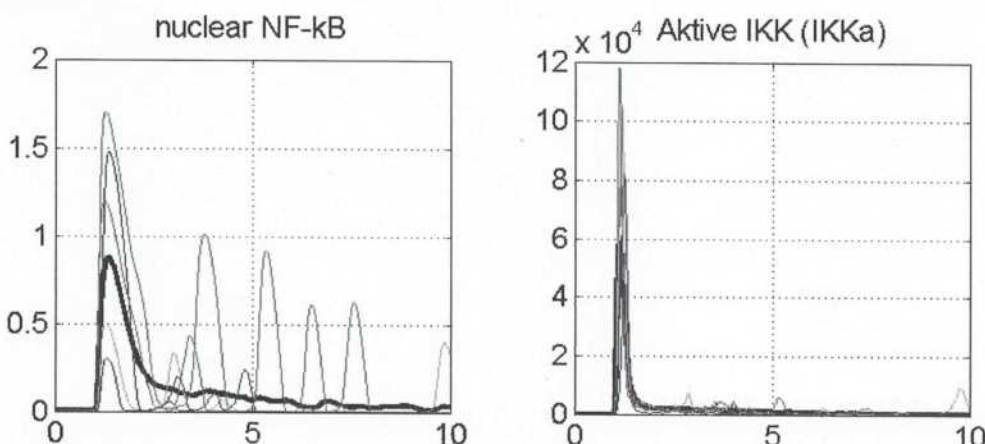
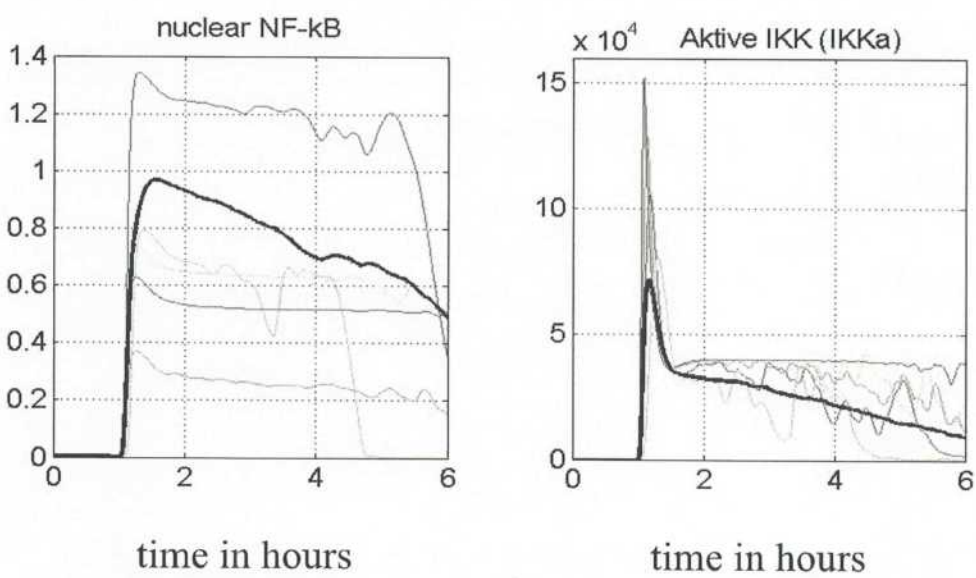
A20 $^{-/-}$ cells

Fig. M6 Active IKK and nuclear NF-κB profiles in wild type and A20 $^{-/-}$ MEFS (10000) under tonic TNF α 1ng/ml stimulation. Bold black line: average over 100 cells, thin lines: single cell stochastic trajectories. Nuclear NF-κB is given in 10^5 molecules.

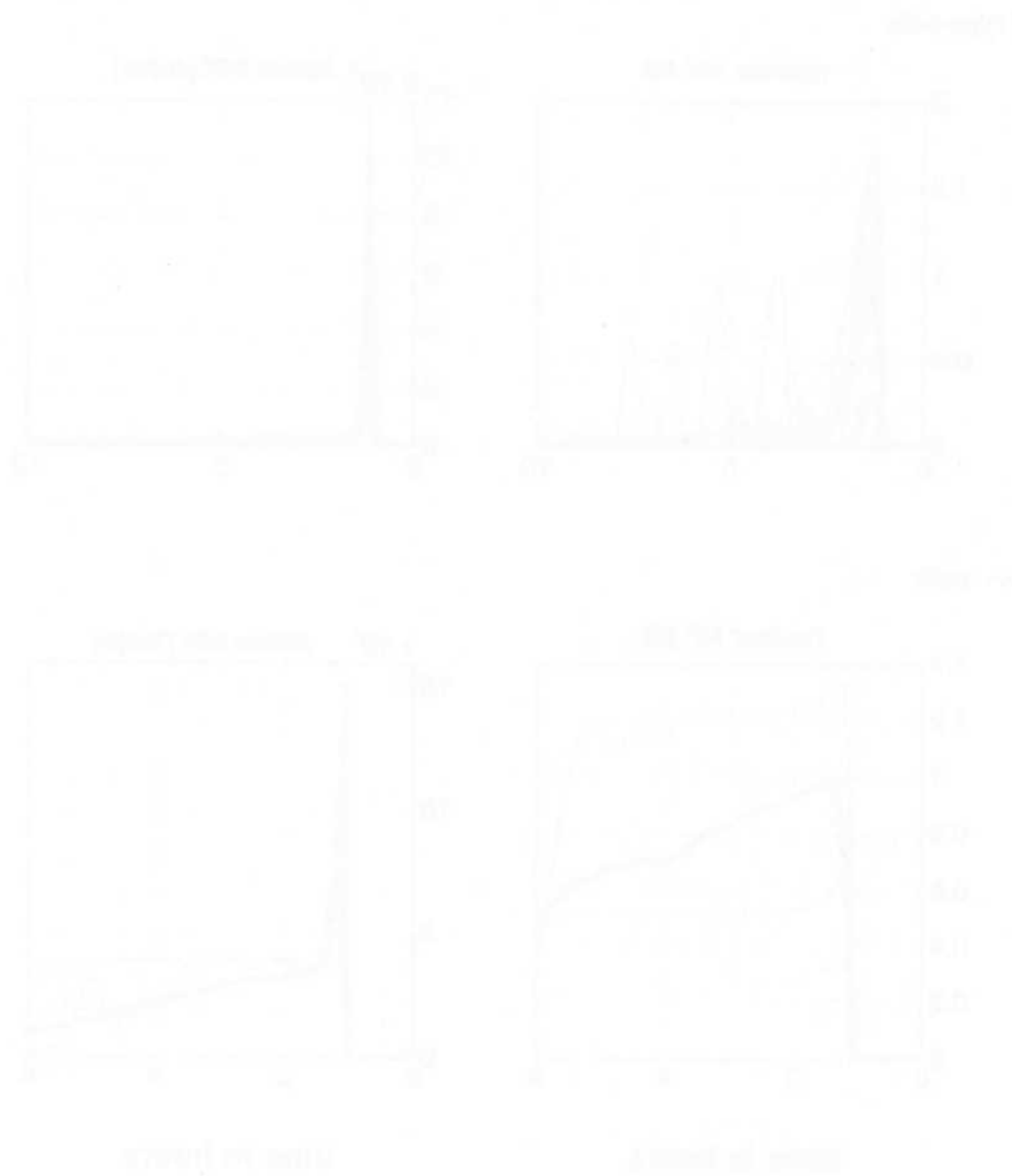


Figure 1. Income-to-needs ratio by age for different income groups. Note: The income-to-needs ratio is calculated as the ratio of income to the poverty line for each household size and composition. The income-to-needs ratio is adjusted for household size and composition using the equivalence scale proposed by the U.S. Bureau of the Census. The income-to-needs ratio is also adjusted for family size using the U.S. Bureau of the Census equivalence scale. The income-to-needs ratio is also adjusted for family size using the U.S. Bureau of the Census equivalence scale.

Table 3 Response to pulse-pulse TNF stimulation (20 min pulse – 180 min break – 20 min pulse). B – fraction of cell responding to both pulses, F – fraction of cells responding to first pulse only, S – fraction of cells responding to second pulse only. Cells in which peak of nuclear NF- κ B exceeds $0.2 \text{ NF-}\kappa\text{B}_{\text{tot}} = 2 \times 10^4$ are considered responding.

TNF dose	Type of model					Experiment
	deterministic	extrinsic noise only	intrinsic noise only	Full model		
0.05ng/ml	B=0.0% F=0.0% S=0.0%	B=2% F=1% S=0.0%	B=5% F=23% S=19%	B=6.5% F=10% S=7.5%	B=8% F=8% S=6%	
0.1ng/ml	B=0.0% F=0.0% S=0.0%	B=7% F=2% S=0.0%	B=18% F=29% S=23%	B=12% F=12% S=11%	B=11% F=10% S=9%	
0.2ng/ml	B=0.0% F=100.0% S=0.0%	B=16% F=4% S=%	B=53% F=22% S=20%	B=22% F=14% S=13%	B=17% F=9% S=5%	

In the deterministic model there exists threshold dose for cell activation, Th1≈0.2 ng/ml above which cells respond to first peak only, and Th2≈0.25 ng/ml above which cells respond to both pulses. Since the response to first peak results in elevated A20 and I κ B α levels cells are slightly more resistant to the second pulse and thus Th2>Th1.

In the extrinsic noise model cell responses are highly correlated, there are very few cells responding to first peak only and none of cells respond to the second pulse only.

In the intrinsic noise model cell activation at both pulses is almost independent and thus

$$B \approx (F + B)(S + B)$$

References

Ashall, L. et al., Pulsatile stimulation determines timing and specificity of NF- κ B-dependent transcription. *Science* 2009, **324**:242-246.

Chan, F. K-M., Three is better than one: Pre-ligand receptors assembly in the regulation of receptors signaling *Cytokine* 2007, **37**:101-107.

Covert, M.W., Leung, T.H., Gaston, J.E., & Baltimore, D., Achieving stability of lipopolysaccharide-induced NF- κ B activation. *Science* 2005, **309**: 1854-1857.

Delhase M, Hayakawa M, Chen Y, Karin M: Positive and negative regulation of I κ B α kinase activity through IKK. *Science* 1999, **284**:309-313.

Fujarewicz K, Kimmel M, Lipniacki T, Swierniak A, Adjoint systems for models of cell signaling pathways and their application to parameter fitting. *IEEE/ACM Transactions on*

Computational Biology and Bioinformatics 2007, **4**:322-335.

Grell M, Wajant H, Zimmermann G, Scheurich P: The type 1 receptor (CD120a) is the high-affinity receptor for soluble tumor necrosis factor. Proc Natl Acad Sci USA 1998, **95**:570-575.

Haseltine EL, Rawlings JB: Approximate simulation of coupled fast and slow reactions for stochastic chemical kinetics. J Chem Phys 2002, **117**:6959-6969.

Hoffmann A, Levchenko A, Scott ML, Baltimore D: The I κ B α - NF- κ B signaling module: Temporal control and selective gene activation. Science 2002, **298**:1241-1245.

Krikos A, Laherty CD, Dixit VM: Transcriptional activation of the tumor necrosis factor alpha-inducible zinc finger protein, A20, is mediated by kappa B elements. J Biol Chem 1992, **267**:17971-17976.

Lipniacki T, Paszek P, Brasier AR, Luxon B, Kimmel M: Mathematical model of NF- κ B regulatory module. J Theor Biol 2004, **228**:195-215.

Lipniacki T, Paszek P, Brasier AR, Luxon B, Kimmel M: Stochastic regulation in early immune response, Biophys J 2006, **90**:725-742.

Lipniacki, T., Puszynski, K., Paszek, P., Brasier, A. R., Kimmel, M. Single TNF- α trimers mediating NF- κ B activation: Stochastic robustness of NF- κ B signaling. BMC Bioinformatics 2007, **8**:736-756.

Lee EG, Boone DL, Chai S, Libby SL, Chien M, Lodolce JP, Ma A: Failure to regulate TNF-induced NF- κ B and cell death responses in A20-deficient mice. Science 2000, **289**:2350-2354.

Nelson DE, et al.: Oscillations in NF- κ B signaling control the dynamics of gene expression. Science 2004, **306**:704-708.

Schomer-Miller B, Higashimoto T, Lee Y-K, Zandi E: Regulation of I κ B α kinase (IKK) complex by IKK -dependent phosphorylation of the T-loop and C terminus of IKK. J Biol Chem 2006, **281**:15268-15276.

Werner SL, Barken D, Hoffmann A: Stimulus specificity of gene expression programs determined by temporal control of IKK activity. Science 2005, **309**:1857-1861.

Werner, S. L., Kearns, J. D., Zadorozhnaya, V., Lynch, C., O'Dea, E. L., Boldin, M. P., Ma, A., Baltimore, D., Hoffmann, A. Encoding NF- κ B temporal control in response to TNF: distinct roles for the negative regulators I κ B α and A20. Genes and Development, 2008, **22**:2093-2101

Wertz IE, O'Rourke, KM, Zhou H, Eby M, Aravind L, Seshagiri S, Wu P, Wiesmann C, Baker R, Boone DL, Ma A, Koonin EV, Dixit VM: De-ubiquitination and ubiquitin ligase domains of A20 downregulate NF- κ B signaling. Nature 2004, **430**:694-699.

Zhang SQ, Kovalenko A, Cantarella G, Wallach D: Recruitment of the IKK signalosome to the p55 TNF receptor: RIP and A20 bind to Nemo (IKK) upon receptor stimulation. Immunity 2000, **12**:301-311.

